

**STATISTICAL THERMODYNAMICS OF HIGH T_c TWO BAND
SUPERCONDUCTIVITY IN MgB_2**

Igunza Edward Salano

**A thesis submitted in partial fulfillment of the requirements for the award of the degree of
Master of Science in Physics of Masinde Muliro University of Science and Technology.**

OCTOBER, 2019

DECLARATION

This thesis is my original work, prepared with no other than the indicated sources and support and has not been presented elsewhere for a degree or any other award.

Sign: Date:.....

Igunza Edward Salano

Reg No: SPH/G/02/15

Approval

The undersigned certify that they have read and hereby recommend for acceptance of MasindeMuliro University of Science and Technology a thesis entitled:

“Statistical Thermodynamics of High Tc two band Superconductivity in MgB₂”.

Sign:..... Date:.....

Dr. NdinyaBonface

Department of Physics,

MasindeMuliro University of Science and Technology.

Sign:..... Date:.....

Dr. RapandoWakhu.

Department of Physics,

MasindeMuliro University of Science and Technology.

COPYRIGHT

This thesis is copyright materials protected under the Berne convention, the copyright Act 1999 and other international and national enactments in that behalf, on intellectual property. It may not be reproduced in any means in full or in part except for short extracts in fair dealing for research or private study, critical scholarly review or discourse with acknowledgement with written permission of the Director, Directorate of graduate Studies on behalf of both the author and MasindeMuliro University of Science and Technology.

DEDICATION

To my children, Holiness Shakina Salano, Emmanuel Ben Salano, Prosper Eden Salano and my beloved wife Deborah OresiaSalano,whose love kept me going throughout the study.

ACKNOWLEDGEMENT

I sincerely thank the Almighty God for the life, strength, guidance and good health he offered me throughout the study. I extend my gratitude and thanks to my supervisors Dr. Ndinya Boniface and Dr. RapandoWakhu for their valuable sacrifices, suggestions, comments, guidance, providing most of literature and being generous with their time that helped make this research a reality.

ABSTRACT

Thermodynamic properties of the multiband high critical temperature superconductors have been described previously with simple standard BCS expressions corresponding to σ and π bands, but the microscopic mechanisms that allow superconductivity to persist at high temperatures remain unknown. Studies on two band superconductors have previously been described through one band model; this approach has not adequately addressed cases of inter-band scattering for superconductors at high temperature. Research reverted to canonical two band BCS Hamiltonian containing a fermi surface of p- and d- bands, followed by Bogoliubov-Valatin transformation equations, to obtain transition temperature, energy gap and specific heat for MgB_2 superconductor. A detailed study of phonon-mediated attraction and coulomb repulsion was proposed to act differently on energy band states and stabilizing superconductor phase for MgB_2 . The results were compared to the approach of a sum of two independent bands using Bardeen, Cooper and Schrieffer like π - and α - model expressions for the specific heat, entropy and free energy to the solution of Bogoliubov-Valatin transformation for strongly correlated electrons. The research led to development of electron-phonon interaction model Hamiltonian for superconducting MgB_2 and its energy, obtaining transition temperature T_C for MgB_2 superconducting and expression for variation of thermodynamic properties of high T_C superconductors in two-band model system. The research demonstrated the physical meaning of the sum over the contribution of the two bands, where band parameters tend to agree with the previous determinations of band structure calculations and experiments. Information was found on the thermodynamic transition by presenting an empirical two bands that fits the experimental data over the whole range of temperature to high T_C . A perturbed Hamiltonian was developed from the Bogoliubov-Valatin transformations equations, where thermodynamic variables were derived. Kaleidagraph and Mathcad software were used to calculate values of statistical thermodynamics of high T_C variables for high temperature superconductors, which included specific heat capacity = 0.0192729906 eV/K, calculated $T_C = 47.667720441\text{K}$, ground state energy = 0.4111340888 eV, total energy = 0.7670001738 eV and entropy = 3.3245572813 eV/k used in data processing and analysis.

TABLE OF CONTENTS

Declaration	ii
Copyright	iii
Dedication	iv
Acknowledgement	v
Abstract	vi
TABLE OF CONTENTS.....	vii
LIST OF TABLES.....	i
LIST OF FIGURES	ii
Abbreviations and Acronyms	ii
LIST OF SYMBOLS	iii
Definition of terms	vi
CHAPTER ONE	1
INTRODUCTION	1
1.1 Background Information.....	1
1.2 Statement of the problem	5

1.3. Objectives of the study.....	6
1.3.1 General objective	6
1.3.2 Specific Objectives	6
1.4 Significance of the study.....	7
1.5 Scope of the study.....	7
1.6 Assumption and Limitation.....	8
1.7 Dissemination of the results.....	8
CHAPTER TWO	9
LITERATURE REVIEW	9
2.1 Introduction.....	9
2.2 Properties of superconductivity.	11
2.2.1 The electromagnetic properties.....	11
2.2.2 Isotope effect.....	12
2.2.3 Tunneling and Josephson Effect	13
2.2.4 Electromagnetic properties	15
2.3. Models of superconductivity.....	16
2.3.1. Phenomenological Model	16
2.3.2. Gorter-Casimir Model.....	16
2.3.3. London theory.....	18
2.3.4. Ginzburgh-Landau theory.....	19

2.3.5. The microscopic model.....	21
2.4. Magnesium diboride (MgB ₂) and its properties.....	21
2.5. Existence Of Two-Band Energy Gaps In MgB ₂	25
2.6. Theory Of Superconductivity In MgB ₂	27
2.8Order Parameter.....	33
2.9 Density of state and single particle tunneling.....	34
CHAPTER THREE.....	35
RESEARCH METHODOLOGY.....	35
3.1 Introduction.....	35
3.2 derivations of thermodynamic relations.....	35
3.3 approximations and assumptions.....	36
3.4 softwares used.....	37
CHAPTER FOUR.....	38
THEORETICAL DERIVATIONS.....	38
4.1 Thermodynamic Properties of High T _C Superconductors.....	38
4.2 Defining Operators.....	39
4.3 Model Hamiltonian for two band model isotope.....	39
4.4 Mean Field Approximation.....	42
4.5Bogoliubov-ValatinTransformations.....	45
4.6Interaction energy.....	53

1.7 Specific heat capacity.....	57
4.8Somerfield coefficient and entropy.....	58
4.9.Transition temperature T_c	60
4.11. Density of State and Temperature.....	63
CHAPTER FIVE	66
results, analysis and discussion.....	66
5.1 Numerical Calculations and Results	66
5.2. Ground State Energy.....	66
5.3. Specific Heat Capacity Calculations.....	67
5.4. Calculations for Entropy	67
5.5. Predicted and calculated transition temperature T_c	67
5.1.1 Superconducting order parameter	67
5.1.2 Electronic specific heat (C_{es})	70
5.1.3 Density of States, D_n and temperature	74
5.1.4Energy verses temperature.....	78
5.3 Discussion.....	79
CHAPTER SIX.....	80
CONCLUSIONS AND RECOMENDATION	80
6.1 Conclusions.....	80
6.2. Recommendations.....	82

References.....	83
APPENDICES.....	85

LIST OF TABLES.

Table 2.1 List of superconducting parameters of Magnesium Diboride. MgB ₂	27
Table 2.2 Summary of coherence length and London penetration depth for materials.....	33
Table 2.3 Values for various parameters for MgB ₂ system.....	36
Table 2.4 Schematics/table of methods of preparation for MgB ₂	40

LIST OF FIGURES.

Figure 1.1 Crystal structure of Magnesium Diboride MgB_2	25
Figure 1.2: Structure of MgB_2 with B layers separated by hexagonal close-packed layer of Mg.....	26
Figure 5.1 Variation of superconducting order parameter for p and d bands with temperature....	71
Figure 5.2 Variation of Electronic specific heat with temperature for both p and d bands.....	74
Figure 5.3 Variation of density of states function with ω for both p and d bands.....	78
Figure 5.4 Variation of energy verses temperature.....	79

ABBREVIATIONS AND ACRONYMS

BCS Bardeen Cooper Schrieffer

D(E)	Density of state
T	Temperature
T _c	Critical temperature
EM	Electromagnetic field.
DFT	Density function theory
SQUID	Superconducting Quantum Interference Device
RTS	Room Temperature Superconductivity.
HTS	High Temperature Superconductors.
LTS	Low Temperature Superconductors
BEC	Bose Einstein Condensate

LIST OF SYMBOLS

MgB₂ Magnesium Diboride

C	Heat Capacity
T	Thermodynamic Temperature
H	Hamiltonian operator
ρ_i	Probability density operator
S	Entropy
E_n	Energy of the system
B_c	Magnetic Induction
J_c	Critical current density
H_o	Critical field at 0K
H_c	Critical field
V_F	Fermi velocity
ξ_o	Coherence length
Sn	Silicon
Al	Aluminum
Pb	Lead
λ_L	London penetration depth
Δ	Energy gap
ψ_r	Wave function
ε_{ds}	Kinetic energy measured to Fermi level with spin in d-band.
ε_{ps}	Kinetic energy measured to Fermi level with spin in p-band.
V_{dkk^1}	Inter-band phonon mediated matrix in d-band.
V_{pkk^1}	Inter-band phonon mediated matrix in p-band

V_{dpkk^1}	Phonon matrix element for combined inter-band interaction.
V_{dd}	Pairing interaction potential in the d-band.
V_{pp}	Pairing interaction potential in the p-band.
V_{dp}	Pairing potential interchange between the d band and p band.
μ	Common chemical potential
ϵ_d	Energy in d band.
ϵ_p	Energy in p band.
C_v	Specific heat capacity at constant volume.
λ	Penetration depth
Δ	Energy gap in superconductor.
DC	Direct Current
S	Entropy
K	Kelvin

CONSTANTS

Quantity	Symbol	Magnitude
Boltzmann constant	K_B	$8.625 \times 10^{-5} \text{eV/K}$
Reduced Plank constant	$\hbar = h/2\pi$	$1.0544 \times 10^{-34} \text{Js}$
Mass of nuclear matter	m	$6.64 \times 10^{-27} \text{kg}$
Pi	π	3.142
Weber's constant	\emptyset	2.07×10^{-15}
Electron charge	e	$1.6 \times 10^{-19} \text{C}$
Scattering length		$1.3 \times 10^{-13} \text{cm}$
Occupational number of states n		0,1,2,...n
Fermion molar mass		$2.80 \times 10^{-30} \text{Kg}$
Boson molar mass		$3.92 \times 10^{-30} \text{Kg}$
Planks constant	h	$6.626 \times 10^{-34} \text{Js}$
Electron Volt	eV	$1.60219 \times 10^{-19} \text{J}$
Angstrong		$1.0 \times 10^{-10} \text{m}$

DEFINITION OF TERMS

Hamiltonian;

This is the total energy function of the system.

Annihilation operator:

It is also called lowering operator, a mathematical operator that lowers the number of particles in a given state by one.

Bose-Einstein condensation:

This is a finite temperature occurrence whose potential goes to zero and there is a macroscopic occupation of the zero-momentum state.

Creation operators:

They are also called raising operators. It is a mathematical operator that increases the number of particles in a given state by one.

Grand canonical ensemble:

This is a collection of particles used to describe an individual system which is allowed to exchange both energy and particles with its environment.

Fermion:

Identical particles with odd sum of (number of particles possessing) half integral spin angular momentum.

Bosons:

Identical particles with (even sum of the number of particles and possesses) integral spin angular momentum, that can occupy single particle state in the ground state.

Hilbert space:

Set of states obtained when creation and annihilation operators act on ground state.

Perturbation theory:

A mathematical tool that give approximate solutions to problems that cannot be solved exactly.

Cooper pair;

Dynamic pairing of two electrons that possesses opposite spin in the condensate state, move together and exhibit bosonic characteristics.

Entropy;

Entropy is a measure of the molecular disorder of a system.

Superconductivity;

A property observed in certain materials where at zero magnetic field strength, the material exhibits zero DC electric resistance to current flow below certain transition temperature T_c .

Specific Heat;

The quantity of heat energy that raises the temperature of a unit mass of a substance by a Kelvin.

CHAPTER ONE

INTRODUCTION

1.1 Background Information

Superconductivity is the property of some materials (metal, metallic alloys and ceramic oxides, etc.) characterized by an abrupt and complete disappearance of resistance to direct electrical current when the materials are cooled below a certain temperature known as the critical or transition temperature T_C of the material. Superconductivity is zero direct current electrical resistance and materials exhibiting this phenomenon are called superconductors. Since its discovery by (Onnes, 1911) superconductivity has found many applications in technology which are found in nuclear magnetic resonance, tomography, magnetic sensors (magnetometer), digital signal and data processing (geological survey), superconducting magnetic levitated train, superconducting magnet used to detonate mines, superconducting cables, superconducting magnetic energy storage (SMES) etc.

However, these applications of superconductivity have been constrained by the need to maintain their low temperature with refrigerant liquid helium. Consequently, physicist and material scientist have been working relentlessly to improve the temperature nature of this phenomenon and obtain superconductivity at high temperatures. (Mathias, Geballe, & Corenzwit, 1950) Pioneered the search for the high T_C superconductors in transition metal alloys and compounds. This led to independent discovery of superconductivity in thin films of the A12 compound Nb_3Ge at 23K. Superconductivity has been discovered in several other classes of materials such as the cheveral phases, heavy fermion systems, organic superconductors and more recently diborides. The cheveral phases $A_xMO_6X_8$ are mostly ternary transition metals

chalcogenides where X is Sulphur (S) selenium (Se) also A and M can be any element. According to (Allan, 2013) The study of heavy fermion system led to discovery of $CeCu_2Si_2$ systems. Heavy Fermion system often exhibit two ordering transitions, a superconducting transition at T_C and antiferromagnetic ordering transition at Neel temperature. In 1986, Bednorz and Muller, reported observation of superconductivity with $T_C = 30K$ in the ternary $(La_{1-x}Ba_x)_2CuO_4$ otherwise known as 214 compounds. Before the end of 1986, superconductivity at up to 57K in La-Ba-Cu-O under pressure and improved stoichiometry was reported. It was found that T_C of La-Ba-Cu-O increases with pressure at unprecedented rate. The search for new high temperature superconductors has proceeded by following simple trends in the periodic table which provide insight into the correct theoretical model for the superconductors in the light of this tremendous progress made in raising transition temperature of the copper oxide superconductors, it's natural to know how high the T_C can be increased in other classes of materials. The discovery of superconductivity with $T_C = 39K$ in Magnesium diboride (MgB_2) by (Akimitsu, 2001) caused excitement in the solid-state physics because it introduced a new simple binary intermetallic superconductor with a record high superconducting T_C for non-oxide and non C_{60} based compound.

The first classes of high temperature superconductors were discovered in 1986 by Bednorz and Mueller. Although they were awarded Nobel prize in physics in 1986, the microscopic mechanisms that allow superconductivity to persist at such high temperatures remained unknown. Wide explanations have been offered but it's now generally accepted that as in conventional superconductors, the superconducting state is caused by the formation of Cooper pairs, with opposite spin. The cuprates phase diagram have universal features independent of the chosen

compound whose parent compound is the Mott insulator. In hole-doped superconductors, the antiferromagnetic state associated with the Mott insulator according to (Bednorz & Mueller, 1986), persists over small ranges of relatively high temperature where the superconducting state emerges as a dopant concentration increases and the antiferromagnetic state disappears. The superconducting state persists over wide range of dopant concentration and the material is said to be optimally doped when it achieves its maximum T_C below or above that dopant concentration and is said to be under or over doped respectively. (Bednorz & Mueller, 1986) showed that critical temperature decreases in case of MgB_2 due to Al or C doping which was mainly explained as due to a simple effect of band filling. Further, the doping independent π -gap in C-doped MgB_2 can be understood as due to a compensation of band filling and inter-band scattering effects.

MgB_2 has large coherence length, high critical current densities and field; therefore, it may be a preferable one as the best superconductors in the present scientific world. Superconductivity has several technical applications and is under active study around the world hence need for the research. (Choi, Roundy, Sun, & Cohen, 2002) and (Bednorz & Mueller, 1986) discovered high temperature superconductors that could work under high temperatures. High critical temperature superconductors are characterized by 1-2-3 compounds, perovskite crystal structure, which is a calcium titanium oxide mineral composed of calcium with directional dependent, oxides of Cu^+ and other elements. Major development has been made in discoveries of higher temperature superconductors as well as progress in the theory of superconductivity. American physicists John Bardeen, Leon Cooper and Schrieffer (BCS) on superconductivity made advancements in 1957 where boson like behavior of electron pairs were investigated, a passing electron attracts the lattice, causing a slight ripple in its path, which was known as BCS theory and won them a Nobel

Prize in 1972. Bardeen, Cooper and Schrieffer theory explained superconductivity at temperatures close to absolute zero for elements and simple alloys. However, according to (Akimitsu, 2001) discovered BCS theory has become inadequate to fully explain how superconductivity occurs at higher temperatures and with different superconductor. More advancement has been made in improving the area by predicting and engineering new types of superconductors, in 1980s carbon-based superconductors were found to have good magnetic properties and high critical temperatures with mechanical properties.

According to (Bednorz & Mueller, 1986) and (Keimer, Kivelson, Norman, & Uchida, 2015), discovery of high T_C superconductivity at relatively high temperature has appealed attention in theoretical and applied condensed matter physics. The compounds have been called the first superconductor with two energy bands at the Fermi surface in two dimensional bands with Inter-band scattering between them being negligible. In exploring the mechanism of superconductivity in MgB_2 compound, it was crucial to determine the symmetry of superconducting order parameter which governs the behavior of quassiparticle excitation. According to (Mourachkine, 2004) When exposed to neutron irradiation, such samples exhibit considerably reduced critical temperature, while the two bands persist even at very low critical temperatures. extensively studied thermodynamic properties of anisotropic superconductors in the weak coupling regime, BCS model was extended showing the specific heat jump at critical temperature was reduced as compared to the isotropic case.

For two-band weakly coupled superconductors, the specific heat was calculated and the main prediction was that at T_C the relative jump in the electronic specific heat, $(C_{sc}-C_N)/C_N$, where

(C_{sc} refers to superconducting state and C_N refers to normal conducting state) is reduced as compared to the universal BCS value of 1.43 (Bednorz & Mueller, 1986). On the other hand, for an isotropic strongly coupled superconductor the relative specific heat jump is larger than 1.43. The combined effect of strong coupling and multiband anisotropy on the specific heat was studied earlier by (Legget, 2006) where the results of the first principles calculations of the electron-phonon interaction in MgB_2 were used. However, the effect of inter-band impurity scattering was not considered. The results are applied to MgB_2 using the first principles band-structure results or Pauli exclusion principle that dictates a number of electrons in a band structure for the electronic spectra and electron-phonon interaction by extending our preceding approach. The superconducting energy band, the free energy, the entropy and the heat capacity for varying nonmagnetic inter-band scattering rates will be considered within the framework Bogoliubov-Valatin canonical transformation equation (Bogoliubov & Valatin, 1958). The expression for the thermodynamic potential on the extremal trajectory corresponding to solutions of the Bogoliubov-Valatin transformation equations will be compared with sum of contributions of σ - and π -bands, taking into consideration that the total thermodynamic potential has physical meaning.

1.2 Statement of the problem

Studies on two band superconductors by electron spectrum between effective band systems in MgB_2 exhibited characteristics whose theoretical results were compared to experimental data, (Schrieffer, 2013). Experimental results in MgB_2 indicated existence of a d-wave and p-wave superconducting band gap, such pairing in heavy fermions is not yet established and specific superconducting thermodynamic properties are not clearly stated; (Allan, 2013). Properties of the

two-band superconductors at high critical temperature have been described by simple sum of the standard BCS corresponding to α - and π - bands, but the microscopic mechanisms that allow superconductivity to persist at such high temperatures remains unknown. Measurements for components of complex superconductivity of MgB₂ film, a function of frequency for different temperatures was done and results compared with conventional superconductors which were found to be inconsistent with BCS calculations due to additional absorption, (Kaindl, et al., 2001). Other authors were limited to using electron-phonon interactions between effective bands and a recommendation made for more study to be done (Sethna, 2012). The current research reverted to canonical two bands BCS Hamiltonian containing a fermi surface of p- and d- bands with inter-band coupling followed by Bogoliubov-Valatin transformation equations. A detailed study of phonon-mediated attraction and coulomb repulsion was proposed to act differently on energy band states and stabilizing superconductor phase by applying Bogoliubov-Valatin transformation equation to get analytical equations, whose results were compared to the plane wave BCS pseudo potential method based on electron-phonon interactions in obtaining thermodynamic properties of MgB₂.

1.3. Objectives of the study

1.3.1 General objective

To determine thermodynamic properties of high T_C superconductors in two band model using electron-phonon interactions between effective two bands system.

1.3.2 Specific Objectives

- (i) To develop electron-phonon interaction model Hamiltonian for superconducting MgB₂.
- (ii) To obtain transition temperature, T_C equation for MgB₂ superconducting system.

(iii) To obtain expression for variation of thermodynamic properties entropy, transition temperature, specific heat capacity Sommerfeld coefficient and electronic specific heat with temperature.

1.4 Significance of the study

Superconductivity promotes activities that cover the science and technology of superconductors and their applications. Area of interest ranges from small scale application, such as ultra-sensitive radiation detectors, sensors, analog and digital circuit systems. Also, large scale applications such as high field magnets and electrical power generating storage and transmission. The development and enhancement of the properties of superconductor materials suitable for the use of these applications is also of great concern. Magnesium Diboride (MgB_2) has been found to have its superconductivity at $T_c = 39\text{K}$ (Tinkham, 2004). According to Tinkham, intermetallic MgB_2 has the highest critical temperature at ambient pressure among all superconductors with exception of cuprates. It has large coherence length, high critical densities and field therefore, it is a preferably one of the best superconductors in the present scientific world.

1.5 Scope of the study.

The study explored MgB_2 theoretically using Bogoliubov-Volatin Canonical transformations for both an isotropic one-band model with different superconducting bands at Fermi surface. This lead to expressing variation of thermodynamic properties of high T_C superconductors in two band model using electron-phonon interactions between effective bands in two bands system in MgB_2 . In addition, superconductivity of MgB_2 was studied, by mentioning experiments to motivate theoretical ideas, support or contradict theoretical predictions and systematic discussions. The study used the knowledge of standard material from electrodynamics,

thermodynamics and second quantization formalization of creation and annihilation operators in construction of electron-phonon interaction model Hamiltonian of the system of MgB₂. The study then applied first-principles calculations with the Coulomb repulsion to obtain variation of thermodynamic properties with temperature in MgB₂ and other objectives.

1.6 Assumption and Limitation.

Inter-band scattering is expected to modify T_C and density of states strongly for MgB₂. This will help to calculate T_C , the gap functions and the superconducting density of states by analyzing nonlinear equations for various values of inter-band nonmagnetic scattering rates. These results demonstrated the self-energy effects arising due to the sizable electron-phonon interactions in MgB₂ with characteristic phonon frequencies.

1.7 Dissemination of the results

This research will be of great use to theorists and experimentalists, who intend to contribute to this rapidly growing area of Condensed Matter Physics. The results of this work will be disseminated through seminars, publications in local and international journals and oral presentations of this thesis before the board of School of Graduate Studies in Masinde Muliro University of Science and Technology.

CHAPTER TWO

LITERATURE REVIEW

2.1 INTRODUCTION

(Bednorz & Mueller, 1986) studied the mechanisms that allow pairing in the cuprate superconductors at high T_C and did not get clear consensus. They came up with qualitative results for DC SQUIDS measurements, with d-wave pairing states being dominant in the cuprates.

(Bednorz & Mueller, 1986) also discovered and studied the cuprates first class of high temperature superconductors and were awarded the Nobel Prize in physics, but the microscopic mechanism that allows superconductivity to persist at high temperatures remained undefined. The high transition temperature of 40K in two-band superconductivity was the unexpected phenomenon in MgB_2 which attracted increasing attention. At present, it appears that the MgB_2 is among superconductors with substantiated theoretical and experimental evidence for two-band superconductivity. Two band superconductivities have been investigated theoretically after the formulation of BCS theory.

Suhl, (Hensen, Mueller, Riek, & Scharnberg, 1997) who suggested a model for transition metals considering overlapping s- and d-bands and proposed an extension of the BCS theory for multiple bands that lead to a review of theoretical treatment of the critical temperature T_C of multiband superconductors being found. MgB_2 appeared to be the first system to which multiband superconductivity has independently been evidenced by several experimental techniques like Raman spectroscopy, heat capacity, tunneling spectroscopy and penetration depth measurements with the analysis of the critical field. The theoretical justification for two

band superconductivity in MgB_2 has been given from the electronic structure calculations that found that the Fermi surface contained quasi-cylindrical sheets corresponding to nearly two-dimensional bands. A three-dimensional network of the Fermi surface is attributed to the bands and has been demonstrated that the optical bond stretching E_{2g} phonon couple strongly to the holes at the top of σ -bands while the three-dimensional π -electrons couple only weakly to the phonons. The different coupling of the σ - and π - bands lead to the superconducting gaps different in character and size. Using the linear response theory, (Akimitsu, 2001), it is possible to calculate the electron-phonon coupling from Bogliubov and Valatin canonical transformations equation. The superconducting gaps obtained in this method are in very good agreement with the experiments.

There have been several studies to detect the MgB_2 gap. The isotope effect of boron has suggested that MgB_2 is a BCS-type superconductor and the high T_C is realized through strong electron-phonon coupling with light boron mass. (Poole C P Jr, 2000) and (Akimitsu, 2001) Studies have shown two different superconducting gaps, a gap much smaller than the expected BCS value and another is comparable to the BCS given by $2\Delta = 3.53 K_B T_C$. as ratio is estimated to be $\Delta_{\min}/\Delta_{\max} \approx 0.3 - 0.4$ using several experiments. The two-gap model is seen to consistently describe the optical conductivity and thermodynamic properties of MgB_2 , however, there is no general agreement whether MgB_2 is an s-wave BCS type superconductor or not. In conventional s-wave superconductors, there is no quasi particle excitation at low energies and the thermodynamic and transport coefficients decay exponentially at low temperatures. Measurements show that low temperature dependence of penetration depth of MgB_2 behavior disagree with BCS calculations caused by an additional absorption. Also, additional theoretical

calculations of (Mathias, Geballe, & Corenzwit, 1950) show that the penetration depth is well described by two band models as the measured components of complex conductivity of MgB₂ film which has a function of frequency for different temperatures. Their results were compared with conventional superconductors and concluded that they were inconsistent with BCS results, which was caused by additional absorption.

2.2 Properties of superconductivity.

Superconductors have peculiar properties which are distinguished from normal conducting state by electromagnetic, thermodynamic, Isotope effect, tunneling effect among others.

2.2.1 The electromagnetic properties

According to (Keimer, Kivelson, Norman, & Uchida, 2015) showed that similar to the electromagnetic properties such as Gibbs free energy, entropy and electronic specific heat of a metal, they also change sharply at the transition temperature for superconductivity.

In a magnetic field, the Gibbs free energy of a system is given by

$$G(P, T, S) = U - TS - MH \quad (2.10)$$

Where U is the internal energy, S is the entropy, M is the magnetization, P is the pressure and T is the absolute temperature. When internal energy is fixed then

$$dG = SdT - MdH \quad (2.11)$$

In normal metal, G_n is independent of H, then

$$dG_n = -S_n dT \quad (2.12)$$

In a superconductor

$$dG_s = -SdT - (-H)dH \quad (2.13)$$

Entropy in the superconducting state is always less than the entropy in the normal state. (Tinkham, 2004) observed that the transition to the superconducting state is accompanied by a slight jump in the specific heat. The transition from the superconducting state to normal state is second order in zero magnetic field at $T_c=T$. This means that there is no discontinuity at T_c in either entropy or thermal hysteresis, but there is a sharp discontinuity in the heat capacity. (Poole C P Jr, 2000) The specific heat in the normal state varies linearly with temperature T , while specific heat in the superconducting state initially shoots above normal state C_n , and drops below it before finally vanishing exponentially as $T \rightarrow 0$. Theoretically, it is found that the specific heat below T_c , C_s is given by (Poole C P Jr, 2000) as

$$C_s \approx \exp\left(\frac{-\Delta}{K_B T}\right) \quad (2.14)$$

where Δ is the energy gap. This dependence indicates the existence of an energy gap in the energy spectrum separating the excited state from the ground state. The presence of an energy gap in the spectrum of the quasi-particles has been observed directly in various other ways. The presence of the energy gap of order T_c explains the absence of thermoelectric effect as postulated theoretically.

2.2.2 Isotope effect

Isotope effect according to (Keimer, Kivelson, Norman, & Uchida, 2015), it is a property of superconductivity that helps in understanding the roles of phonons in superconductivity. At zero temperature, the critical field and transition temperature T_c vary with the isotopic molar mass of the material as

$$T_c \propto M^{-\beta} \quad (2.15)$$

Where M is the ionic mass of the material, β is the isotope effect exponent. The isotope effect is given as

$$\beta = \frac{\partial \ln T}{\partial \ln M} \quad (2.16)$$

This is for single component system. For multicomponent system, the total isotope effect exponent is the sum of the individual atoms with mass M

$$\sum_i \beta_i = \sum_i \frac{\partial \ln T}{\partial \ln M} \quad (2.17)$$

It has been found that $\beta \approx 0.45 - 0.5$ for many superconductors. The discovery of isotope effect indicates the importance of electron-phonon interaction which provides the basis for the microscopic theory.

2.2.3 Tunneling and Josephson Effect

We considered two metals separated by an insulator that acts as a barrier to flow of conduction electrons from one metal to another. If the barrier is sufficiently thin, ie less than 10 Angstroms, there is a significant probability that an electron which impinges on the barrier will flow from one metal to the other, which is referred to as tunneling effect.

If both metals are superconductors, according to (Tinkham, 2004) two types of particles may tunnel; single quassi-particle and paired superconductor pair. Tunneling of single quassi-particle has been used to measure the energy gap in the superconducting state. Tunneling of superconducting particles is called Josephson Tunneling, it exhibits unusual quantum effect that has been exploited in a variety of quantum devices. The effects of superconductive pair tunneling include

2.2.3.1 DC Josephson effect.

A direct current flows across the junction in the absence of an electric or magnetic field. The current J , of the superconducting pair according to (Keimer, Kivelson, Norman, & Uchida, 2015) depends on the phase difference φ given us

$$J = J_0 \sin \varphi = J \sin(\theta_2 - \theta_1) \quad (2.18)$$

Where J_0 is the maximum zero voltage current that can be passed by the junction. With no applied voltage, a dc current will flow across the junction with the value of J according to the phase difference $(\theta_2 - \theta_1)$.

2.2.3.2 AC Josephson effect

When the current supplied by an external source exceeds the critical value I_c of a superconductor, it causes a voltage V to appear across the junction (Keimer, Kivelson, Norman, & Uchida, 2015). Thus the current of normal electrons I_n starts flowing through the Josephson junction. This leads to resistively shunted model of the Josephson junction (RSJ) which is considered as a circuit made up of Josephson junction itself and normal resistance connected in parallel. The total current is then the sum of the normal current and the super current. Where R is the normal state resistance of the junction. The presence of the voltage V across the weak link suggests that Cooper pair energies in superconductors on either sides of the junction E_1 and E_2 are related by

$$E_1 - E_2 = 2eV \quad (2.19)$$

Hence the second fundamental relation of Josephson with frequency is

$$\omega = \frac{2e}{\hbar} R \sqrt{I^2 - I_c^2} \quad (2.20)$$

This is a fascinating property of Josephson junction.

The frequency of the AC voltage depends on the amount by which the current through the junction exceeds the critical value. The first experimental observation of the Josephson radiation was reported in 2006.(Martins, 2006).

2.2.4 Electromagnetic properties

Electromagnetic properties of superconductors were first observed experimentally by (Martins, 2006), showed the disappearance of electrical resistance of some metals i.e. mercury, lead, tin etc and alloys in small range of temperature around critical temperature T_C , characteristic of the material. Critical temperatures for typical superconductors range from 4.15K for mercury to 3.9K for tin, 7.2K and 9.2K for lead and niobium respectively. This is particularly clear in experiments with persistent current in superconducting rings as a result of zero resistance leading to infinite conductivity. This current was observed to flow with unmeasurable decay up to 10^5 years. Good conductors have resistivity at a temperature of several degrees kelvin of the order of $10^6 \Omega \text{cm}$.

(Choi, Roundy, Sun, & Cohen, 2002), In 2002 Meissner and Ochenfield discovered a scenario of perfect diamagnetism, where the magnetic field operated only at a depth $\lambda \approx 500$ Angstroms and is excluded from the body of the material. Due to vanishing of the electrical resistance, the electrical field is zero within the material, therefore as to the Maxwell equation where C_1 is the current. Hence

$$\nabla X E = \frac{-1}{C_1} \frac{\partial B}{\partial t} \quad (2.21)$$

The magnetic field is frozen, but it is expelled. This implies that the superconductivity will be destroyed by a critical field H_C such that

$$f_s(T_C) + \frac{H_C^2}{8\pi} = f_n(T_C) \quad (2.22)$$

Where $f_{s,n}(T_c)$ are the densities for free energy at superconducting phase at zero magnetic field and in the normal phase. The behavior of the critical magnetic field with the temperature was found empirically to be a parabolic and by Tuyn's law:

$$H_C(T) \approx (0) \left[1 - \left(\frac{T}{T_C} \right)^2 \right] \quad (2.23)$$

According to (Martins, 2006), the critical field at zero temperature is of order of hundred gauss for type I (soft) superconductor and for hard or type II superconductors, stays up to the value of 10^5 gauss. Above H_{c1} , the magnetic flux penetrates into the bulk of the material in the form of Vortices (after Abrikosov Vortices) and the penetration is complete at $H=H_{c1}>H_{c2}$, where H_{c2} is the upper critical field. Where H_{C1} and H_{C2} is the critical field in type I and type II superconductors respectively

2.3. MODELS OF SUPERCONDUCTIVITY.

2.3.1. Phenomenological Model

In superconductivity, finite fraction of electrons forms a condensate or macro-electrons (superfluid) capable of motion. The condensation at zero temperature is complete overall volume, but when increasing the temperature part, the condensate evaporates and forms a weakly interacting normal fluid liquid where at the critical temperature, all the condensate disappears, (Bednorz & Mueller, 1986)

2.3.2. Gorter-Casimir Model

Was first formulated in 1934 by Gorter and Casimir according to (Kaindl, et al., 2001) and consists of a simple ansatz for the free energy of the superconductor. Where x represent the

fraction of electrons in the normal fluid and $1-x$ the ones in the superfluid. Gorter and Casimir assumed the following expression for the energy of the electrons

$$F(x, T) = \sqrt{x}f_n(T) + (1 - x)f_s(T) \quad (2.24)$$

With

$$f_n(T) = -\frac{\gamma^2}{2}T^2, f_s(T) = -\beta = \frac{-1}{kT} \quad (2.25)$$

In free energy for the electrons in a normal metal is f_n and f_s will give the condensation energy associated with the superfluid. To minimize the free energy with respect to x , we find the fraction of normal electrons at temperature T as

$$x = \frac{1}{16} \frac{\gamma^2}{\beta^2} T^4 \quad (2.26)$$

At $x=1$, the critical temperature T_c is

$$1 = \frac{1}{16} \frac{\gamma^2}{\beta^2} T^4$$

$$T^4 = \frac{16\beta^2}{\gamma^2}$$

$$\sqrt{T^4} = \sqrt{\frac{\beta^2}{\gamma^2}}$$

$$T^2 = \frac{4\beta}{\gamma} \quad (2.27)$$

Therefore, the fraction of electron at temperature T is

$$x = \left(\frac{T}{T_c}\right)^4 \quad (2.28)$$

The corresponding value of the free energy is

where the free energy gap= condensation energy

The specific heat in the normal phase is

$$C_n = -T \frac{\partial^2 f_n(T)}{\partial T^2} = \gamma T \quad (2.29)$$

Where as in the superconducting phase, it is

$$C_s = 3\gamma T_c \left(\frac{T}{T_c}\right)^3 \quad (2.30)$$

It shows a jump in specific heat and the ratio of the two specific heats at transition is 3.

2.3.3. London theory

Phenomenological description for basic facts of superconductivity is by proposing a scheme base on two fluid model concepts with superfluid and normal fluid densities n_s and n_n that is associated with velocities V_s and V_n where the densities satisfy the following expressions as according to(Poole C P Jr, 2000) ,

$$n_n + n_s = n \quad (2.31)$$

n is the average number per volume and the current densities. This gives the London equation as bellow.

$$\Delta X J_s = -\frac{n_s e^2}{mc} B \quad (2.32)$$

2.3.4. Ginzburgh-Landau theory

Formulation of theory of superconductivity by introducing a complex wave function as an order parameter was done in 1950, by Ginzburgh and Landau. The wave function is related to the superfluid density by

$$n_s = |\psi(r)|^2 \quad (2.33)$$

where r defined as the position of the particle.

(Hensen, Mueller, Riek, & Scharnberg, 1997) They further postulated a difference of free energy between the normal and superconducting phase of the form

$$f_s(T) - f_n(T) = \int d^3(r) \left(\frac{1}{2m^*} \psi^*(r) |\nabla + iAe^*|^2 \nabla(r) + \alpha(T) |\psi(r)|^2 + \frac{1}{2} \beta(T) |\psi|^4 \right) \quad (2.34)$$

where m^* and e^* are the effective mass and charge that turned out to be $2e$ and $2m$ respectively in microscopic theory.

$$|\psi|^2 = -\frac{\alpha(T)}{\beta(T)} \quad (2.35)$$

And free energy density becomes

$$f_s(T) - f_n(T) = \frac{-\alpha^2(T)}{2\beta(T)^2} = \frac{-H_C^2(T)}{8\pi} \quad (2.36)$$

Recalling that in London theory as per (Hensen, Mueller, Riek, & Scharnberg, 1997)

$$n_s = |\psi|^2 \approx \frac{1}{\lambda_L^2(T)} \quad (2.37)$$

We find that

$$\frac{\lambda_L^2(T)}{\lambda_L^2(T_C)} = \frac{1}{n} \frac{\alpha(T)}{\beta(T)} \quad (2.38)$$

Combining the above equations, we get

$$n \propto (T) = \frac{-H_c^2 \lambda_L^2(T)}{4\pi \lambda_L^2(0)}$$

and

$$n^2 \beta(T) = \frac{-H_c^2 \lambda_L^2(T)}{4\pi \lambda_L^4(0)} \quad (2.39)$$

Solving the equation of motion at zero EM field, we obtain the lowest order in free energy that

$$\frac{1}{4m^*|\psi(T)|} \nabla^2 f - f = 0 \quad (2.40)$$

We see that as $\alpha(T) \rightarrow \infty$ for $T \rightarrow T_c$

$$\varepsilon(T) = \frac{1}{H_c(T)\lambda_L(T)} \quad (2.41)$$

The ratio of the two-characteristic length defines the Ginzburgh-Landau parameter

$$k = \frac{\lambda(T)}{\varepsilon(T)} \quad (2.42)$$

The Ginzburgh-Landau theory was able to explain the intermediate state of superconductors in which the superconducting and normal domains coexist in the presence of critical magnetic field.

$$H \approx H_C(2.43)$$

2.3.5. The microscopic model

The microscopic model of superconductors, formulated in 1957 by Bardeen, Cooper and Schrieffer now known as the BCS theory gave a successful of most of the basic features of the superconducting state. The theory was initiated on the idea that the carriers of electric current in a superconductor are bound in pairs of electrons. This bound pairs are formed when the electron-electron phonon mediated interaction is attractive and dominates the screened coulomb interaction of the electron.(Schrieffer, 2013)

The expression for the superconducting transition temperature, T_C is

$$K_B T = 1.14 \hbar \omega_D \exp\left(-\frac{1}{N(0)V}\right) (2.44)$$

where $N(0)$ is the electron density of states, V is the net attractive potential between the electrons and ω_D is the Debye frequency.

2.4. Magnesium diboride (MgB_2) and its properties

Magnesium diboride is a superconductor bounded material which was first synthesized in 1953 but its superconducting properties were discovered later. The discovery of superconductivity in MgB_2 with a T_C at 39K sparked great interest with respect to fundamental physics and practical application of the material. This recent discovery of high temperature superconductor has many similarities with the conventional superconductor with T_C 0-30 K which is understood on the basis of the theory proposed in 1957 by Bardeen, Cooper and Schrieffer known as BCS theory of superconductivity. Magnesium diboride is an inexpensive and simple superconductor. Its critical

temperature of 39K is the highest among convectional superconductors and also higher than other cuprates high T_C , where pairing driving force other than phonons have been speculated. Its formation has a hexagonal crystal structure with space group $6mm$ with boron atoms forming graphitelike sheets separated with hexagonal layers of Mg atoms. The boron atoms form honeycombed layers with the magnesium atoms located above the Centre of hexagonal between the boron planes. (Mathias, Geballe, & Corenzwit, 1950) Specific heat together with tunneling spectroscopy measurements as well nuclear magnetic resonance shows MgB_2 as an s-wave superconductor. The phonon density of states of MgB_2 has been obtained by inelastic neutron scattering. Most experiments on MgB_2 such as the presence of isotope effect, T_c pressure dependence indicate that the superconductivity of MgB_2 points towards phonon-mediated BCS electron pairing. The fermi surface of MgB_2 consists of four sheets: two 3D sheets from the π bonding and antibonding and two nearly cylindrical sheets from 2D sigma bonding.

Experiments such as point contact spectroscopy, specific heat measurement, scanning tunneling and Raman spectroscopy as per and (Keimer, Kiverson, Norman, & Uchida, 2015) clearly explains the existence of two distinct superconducting gap with small gaps. Both gaps close near the bulk transition temperature $T_c=39K$ and two distinct superconducting gaps, MgB_2 serves as an important test case for density functional theory (DFT) for superconductors. For simple BCS metal the critical temperature decreases under pressure due to the reduced electron-phonon coupling. For magnesium-diboride the transition temperature also decreases with pressure up to the highest pressure studied. Though the T_c decreases with pressure, the superconducting of MgB_2 is up to 40 GPa. Thermal expansion demonstrates the out of plane Mg-B bonds are much weaker than in plane Mg-Mg bonds.

When the band structure calculations are done, it clearly reveals that, while strong B-B covalent bonding is retained, Mg is easily ionized with its two electrons fully donated to B-derived conduction band. We may assume that the superconductivity in MgB₂ is essentially due to the metallic nature of the 2D sheets of boron and the high vibrational frequencies of light boron atoms lead to high T_C of this compound. (Martins, 2006) The coherence length at zero temperature, $\xi(0)$, of the diboride superconductor in the high T_C material is small comparable with interatomic distance with an average value of about 0.49 Angstrom. It was concluded that MgB₂ is an extreme type II superconductor with Ginzburgh- Landau parameter $K=23$. The observed isotope effect is reduced substantially from BCS value of 0.5. In MgB₂ T_C is sensitive to Boron isotopic substitution while Mg isotope does not make significant change in T_C. According to (Hinks et al 1956) T_c is higher by 1K for Mg¹⁰B₂ compared to Mg¹¹B₂. The Boron isotope coefficient (α_B) is significant and Mg isotope coefficient of (α_{Mg}) is very small but still non-zero. Altogether total isotope coefficient is 0.32 for MgB₂ with high Debye temperature of 750K. Optical measurements and specific heat measurement for MgB₂ estimated $\frac{2\Delta_0}{K_B T_C} \approx 2.6$ which deviates from the BCS value of 3.53.

MgB₂ material is a solid metallic superconductor and made of very light and cheap materials. Its metal has no high contact resistance between the grain boundaries thereby eliminating the weak link problem that avoided the widespread commercialization of temperature cuprate superconductors. For the case of the cuprates, MgB₂ is considered to be having lower anisotropy, larger coherence length, transparency of the grain boundaries to current flow makes it good candidate for application according to (Keimer, Kiverlson, Norman, & Uchida, 2015). MgB₂ has higher prospects of operating temperature with higher device speed than the present electronics

based on Nb. Moreover, higher critical current densities can be achieved in magnetic field by oxygen alloying and irradiation shows increase in current density values. The discovery of MgB_2 superconductivity has spurred the search for other related MgB_2 superconductors.

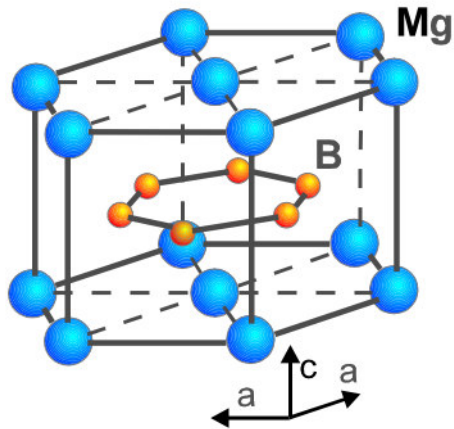


Figure 1.2 Structure containing B layers separated by hexagonal packed layers of Mg for MgB_2

Table 2.1: List of Superconducting parameters of MgB₂. Data review by(Keimer, Kiverlson, Norman, & Uchida, 2015)

Parameter	Values
Critical Temperature	$T_C = 39\text{K}-40\text{K}$
Hexagonal Lattice Parameters	$a = 0.3086\text{nm}, c = 0.3524\text{nm}$
Theoretical Density	$\rho = 2.5\text{g/cm}^3$
Pressure Coefficient	$dT_C / dP = -1.1 - 2\text{K/GPa}$
Carrier Density	$n_s = 1.7-2.8 \times 10^{23} \text{ holes/cm}^3$
Isotope effect	$\alpha_T = \alpha_B + \alpha_{Mg} = 0.3+0.02$
Resistivity near T_C	$\rho(40\text{K}) = 0.4 - 0.6 \mu\Omega\text{cm}$
Resistivity ratio	$RR\rho/\rho(300\text{K}) = 1-27$
Upper critical field	$H_{c2} // ab(0) = 14 - 39 \text{ T}$ $H_{c2} // c(0) = 2 - 24\text{T}$
Lower critical field	$H_{c1} (0) = 27 - 48\text{mT}$
Irreversibility field	$H_{irr} (0) = 6 - 35\text{T}$
Coherence lengths	$\xi_{ab} (0) = 3.7 - 12 \text{ nm}$ $\xi_c (0) = 1.6 - 3.6 \text{ nm}$
Penetration depths	$\lambda(0) = 85 - 180\text{nm}$
Energy gap	$\Delta(0) = 1.8 - 7.5 \text{ meV}$
Debye temperature	$\theta_D = 750 - 880\text{K}$
Critical current densities	$J_c (4.2\text{K}, 0\text{T}) > 10^7 \text{ A/cm}^2$ $J_c (4.2\text{K}, 4\text{T}) = 10^6 \text{ A/cm}^2$ $J_c (4.2\text{K}, 10\text{T}) > 10^5 \text{ A/cm}^2$ $J_c (25\text{K}, 0\text{T}) > 5 \times 10^6 \text{ A/cm}^2$ $J_c (25\text{K}, 2\text{T}) > 10^5 \text{ A/cm}^2$

2.5. Existence Of Two-Band Energy Gaps In MgB₂

A number of experiments contain data with theoretical arguments that favor two gap model superconductivity in MgB₂. Research on the anisotropic superconducting MgB₂ with a combination of scanning tunneling microscopy together with spectroscopy reveal two distinct

energy gaps of 2.3 meV and 7.1 meV according to (Kaindl, et al., 2001). The recent experiments include tunneling spectroscopy, High Resolution Photoemission Spectroscopy (HRPS), Far-Infrared transmission (FIRT) with specific heat treatment points towards the existence of two distinct gaps. Several theoretical researches have used the two-band model to investigate the superconductivity in high T_C superconductors. Fifty years ago Mathias and Walker worked together and predicted the existence of multi gap superconductivity, with a disparity of the pairing interactions in different bands such as p and d bands in transition metals, lead to different order parameters with enhancement of the critical temperature. This scenario was also predicted theoretically by (Akimitsu, 2001) in explaining the magnitude of T_c and to establish the importance of Fermi surface dependent on superconductivity in MgB_2 . Also employed two band models to study isotope effect of high T_c superconductors.

(Bednorz & Mueller, 1986) worked on two band model with superconducting oxide to study isotope effect. He employed use of multi- band superconductors in the case of large disparity of the electron-phonon interaction for different surface sheets. In other cases, such approach has been applied to study the cuprate high T_c superconductivity. First principal approaches showed the Fermi surface of MgB_2 consisting of 2D cylindrical sheets that arise from sigma antibonding states of Boron P_{xy} orbitals and 3D tabula networks arising from pi bands and anti-bonding states of P_z orbitals. In this theoretical framework, two different energy gaps exist, the small one being an induced gap with 3D bands and the large one associated with the superconducting 2D bands.

2.6. Theory Of Superconductivity In MgB₂

Courtesy: Berkeley Lab News, August 2002

Magnesium diboride (MgB₂) superconducts at 39K, which is the highest known transition temperatures (T_c) of any non cuprate superconductor with two superconducting energy gap(Choi, Roundy, Sun, & Cohen, 2002). Theorists at Lawrence Berkeley National Laboratory and the University of California at Berkeley, calculated the properties of this superconductor from first principles and revealed the secrets of its anomalous behavior. In the August 15, 2002 issue of Nature, reported MgB₂'s odd features arise from two separate populations of electrons -- nicknamed "red" and "blue" -- that form different kinds of bonds among the material's atoms. As well as explaining conflicting observations, their calculations led to predictions subsequently borne out by experiment. Further, they suggest the possibility of creating radically new materials with analogous electronic structure. Bottles of powdered MgB₂ have been sitting on the chemical laboratory shelf since the 1950s, but not until January of 2001 did Japanese researchers announce their discovery that it was a relatively high-temperature superconductor. Like high-T_c superconductors made of cuprate ceramics, MgB₂ is a layered material; while undoped cuprates are insulators at ordinary temperatures, however, MgB₂ is always a metal.

"Structurally, magnesium diboride is almost as simple as pencil lead, graphite," says Louie. "It consists of hexagonal honey-combed planes of boron atoms separated by planes of magnesium atoms, with the magnesium centered above and below the boron hexagons."

The simple atomic structure would prove the key to understanding MgB₂. But in the hundreds of papers produced in the first rush to examine the new superconductor, experimenters using

different techniques found many different, unusual, and sometimes conflicting properties."It was like the blind men looking at the elephant," Cohen remarks. "Everybody who looked at MgB₂ saw a different picture. Some said the superconducting energy gap was this; others said it was that; still others found anomalies in measurements of specific heat."It quickly became apparent that theories developed to explain superconductivity in the layered, high-T_c cuprates would not be helpful in understanding MgB₂. Instead, Louie and Cohen and their colleagues used the well-established Bardeen-Cooper-Schrieffer (BCS) theory to examine the fundamental properties of MgB₂, an effort made possible by a technique Choi developed to solve the BCS equations for materials with complex electronic structure(Tinkham, 2004)

In BCS theory, it is revealed that the electrons overcome their mutual repulsion in forming pairs that move through the material. The vital to the pair formation are the quantized vibrations of the crystal lattice, called phonons. If you think of a lattice of positive ions, we picture them 'pulling' the electrons together into pairs, as vibration moves them toward passing electrons," says Cohen. What was puzzling was that, in BCS theory, the coupling to the lattice required to form an electron pair should be equivalent to the coupling of a single electron emitting and reabsorbing a phonon, giving rise to an enhanced electron mass. But in MgB₂ these two values were apparently different -- a clue that more than one kind of electron might be involved in pairing. So the theorists began with basic considerations of MgB₂'s elemental constituents and layered structure.

"To understand the importance of crystal structure to MgB₂'s electronic states, compare it to graphite," Louie suggests, (Choi, Roundy, Sun, & Cohen, 2002). The hexagonal planes for graphite, where each carbon atom has four valence electrons bonded to three others and occupying all available planar bonding states, the sigma bonds; the remaining electron moves

into orbitals above and below the plane, forming pi bonds. MgB_2 has strong sigma bonds in the planes but weak pi bonds between them, but boron atoms have fewer electrons than carbon atoms, hence not all the sigma bonds in the boron planes are occupied. Because not all the sigma bonds are filled, lattice vibration in the boron planes has stronger effect, which results in the formation of strong electron pairs confined to the planes. The Partially occupied sigma bonds driving superconductivity in a layered structure is the new concepts that appeared from the theoretical research," says Louie. "Our other major finding was that not all the boron electrons were needed in strong pair formation to achieve high T_c .

According to (Allan, 2013) Stated differently, electrons on different parts of the Fermi surface form pairs with different binding energies. The theorists' graph of MgB_2 's extraordinary Fermi surface a way of visualizing the highest-energy states its electrons can occupy clearly shows the two populations of electrons and the different energies needed to break their superconducting pairs a graph that incidentally gives rise to the nicknames "red" and "blue" electrons. Four distinctive kinds of sheets make up the Fermi surface. Two form nested cylinders: these map differently oriented sigma bonds and are colored orange and red to indicate the large amount of energy needed to break these superconducting pairs -- a large superconducting "gap," ranging from 6.4 to 7.2 thousandths of an electron volt (meV) at 4 degrees Kelvin. Two other sheets of the Fermi surface form "webbed tunnels" and represent the pi-bonded electrons; they are colored green and blue to indicate the low energy (1.2 meV to 3.7 meV) required to break superconducting pairs of these electrons at 4 degrees K, constituting a separate superconducting gap.

As per (Kaindl, et al., 2001) This two pair of electrons are coupled and with temperature increase, the superconducting gaps for "red" and "blue" pairs rapidly converge, until at about 39K both vanish, with this temperature, the pairs are broken hence material loses superconductivity. The theoretical calculations for superconducting gaps and their temperature dependence for the electrons made it possible for interpretation of the experimental measurements, including those from electron photoemission, neutron analyses scanning tunneling microscopy, optical studies, heat capacity and infrared studies. Cohen (Choi, Roundy, Sun, & Cohen, 2002) performed their first-principles calculations on supercomputers at the Department of Energy's National Energy Research Scientific Computing Center (NERSC) based at Berkeley Lab and first shared them with the condensed-matter community last fall.

Yet BCS theory contemplated the possibility of materials with multiple superconducting energy gaps early on, and the discovery of MgB_2 raises the possibility that others could be made. Louie and Cohen have long studied the electronic properties of unusual materials incorporating boron, carbon, and nitrogen. MgB_2 offers a new model for layered materials capable of high-temperature superconductivity.

2.7 Coherence length and London penetration depth in superconductivity

From various theoretical and experimental researches of superconductivity, (Choi, Roundy, Sun, & Cohen, 2002) they found two characteristic lengths, the London penetration depth and the coherence length. The London penetration depth means the exponentially decaying magnetic field on the superconducting surface. It is also related to the density of superconducting electrons in a given material. The exclusion of magnetic fields from the interior of the superconductor is called the Meissner effect. An independent characteristic length is called the coherence length

which is related to the Fermi velocity for the given material and the energy band associated with the condensation to the superconducting state. It has to do with the fact that the superconducting electron density cannot change quickly; there is a minimum length over which a given change can be made, lest it destroy the superconducting state. For example, a transition from the superconducting state to a normal state will have a transition layer of finite thickness which is related to the coherence length. Experimental studies of various superconductors have led to the following calculated values for these two types of characteristic lengths.

Table 2.2. Distribution for ratio of Coherence length to London depth of different materials.

(Kaindl, et al., 2001)

Material	Coherence length $\xi_0(\text{nm})$	London penetration depth $\lambda_L(\text{nm})$	Ratio λ_L / ξ_0
Sn	231	35	0.151
Al	1610	16	0.002
Pb	84	37	0.44
Cd	761	109	0.14
Nb	38	40	1.05

The maximum distance up to which the states of pair electrons are correlated to produce superconductivity is called coherence length (Tinkham, 2004). Superconductivity is due to the mutual interaction and correlation of the behavior of electrons which extends over a considerable distance. The paired electrons can be many thousands of atomic spacing of 10^{-6}m apart, pointing to the long-range nature of the correlation. The properties of a superconductor depend on the

correlation of electrons within a volume called a coherence volume. It is because the large number of electrons in such a volume act together in superconductivity that the transition is extremely sharp; otherwise statistical fluctuation would cause broadening. Since the electron states responsible for superconductivity lie within $K_B T_C$ of the Fermi surface, by uncertainty principle, their lifetime τ_s is $K_B T_C \tau_s \cong \hbar$ and hence if v_F is the electron velocity at the Fermi surface, the wave function must extend over a distance

$$\xi_0 = \frac{\hbar v_F}{K_B T_C} = \frac{\hbar v_F}{2\Delta} \quad (2.45)$$

where Δ is the energy gap,

A more refined form of this equation is

$$\xi_0 = \frac{2\hbar v_F}{\pi\Delta} \quad (2.46)$$

According to (Schrieffer, 2013), at absolute zero, the ratio of ξ_0 and London's penetration length for metals varies from 1 to 100. In a normal metal, the free electron wave function can be described as a traveling wave.

Every time a normal electron is scattered, its wave vector k will change, and hence, as the electron travels through the metal, its wave function will undergo many random changes of phase. Knowledge of the phase of the wave function at one point does not help to predict the phase at any other point. A superconducting pair can also be considered to have a wave function which contains a similar phase term, except that now k is the effective combined wave vector of the two electrons. However, because the pair cannot be scattered, the phase difference between r_1 and r_2 will be $K \cdot (r_2 - r_1)$, where r_1 and r_2 are momentum positions, called the phase coherence. Consider a body with a hole such as a ring, placed in a magnetic field. Reducing the temperature below T_c will lead to magnetic flux being trapped in the hole even when the field is withdrawn.

This is because the magnetic field lines cannot pass through the surrounding superconducting material hence remaining where they are. London predicted the trapped flux must be quantized i.e, the flux must be an integral multiple of a fundamental quantum of flux. According to (Allan, 2013) he showed that this quantization of flux is a consequence of the phase relationships of the wave function of the electrons in the presence of the magnetic field; his argument relied on an analysis of the effect of the magnetic vector potential on the wave function. Consider a superconducting ring of inner radius R which has some magnetic flux ϕ , trapped inside it. This flux is obviously produced by persistent current which are circulating on the inner surface of the ring. There must be phase coherence at any point on the inner circumference no matter how many times the pairs circulate, and at any point, the phase must remain constant. Hence the line integral of the phase around the inner circumference must be an integer $(n) \times 2\pi$.

2.8 Order Parameter

According to (Sethna, 2012), refers to the wave function of the superconducting states and most important parameter in superconducting state. Superconducting state is a quantum state occurring on microscopic state. This is the reason why, the superconducting state is characterized by a single wave function ψ_r , any wave function has an amplitude and phase represented according to (Keisuke & Daisuke, 2012)

$$\Psi_r = |\Psi_r| \exp i\theta(r) \quad (2.47)$$

where $\theta(r)$ is the phase.

Order parameter has the following properties.

- It has a complex scale which is continuous in real space.

-Its single valued function at any point, $\psi_{(r)}^* \psi_{(r)}$ can only have one value where $\psi_{(r)}^*$ is the complex conjugate of $\psi_{(r)}$

-In the absence of magnetic field $\psi \neq 0$ at $T < T_C$ and $\psi = 0$ at $T > T_C$

– $\psi = 0$ outside a superconductor.

-The order parameter is usually normalized such that $\psi_{(r)}^* \psi_{(r)}$ gives the number density of cooper pairs at point r.

2.9 Density of state and single particle tunneling.

Detailed experimental information on the excitation spectrum in a superconductor can be obtained from single particle tunneling between a superconductor and either normal metal or the superconductor as according to (Mourachkine, 2004). He assumed that density of states $D(E)$ in the normal state is approximately constant close to the fermi energy. He restricted himself to single-electron tunneling, pair tunneling which lead to the Jesephson effect.

CHAPTER THREE

RESEARCH METHODOLOGY

3.1 INTRODUCTION

This chapter gives an account for the theoretical methods used to obtain thermodynamic relations of superconducting MgB₂. The data generation and analysis are also highlighted and assumptions and approximations are stated.

3.2 DERIVATIONS OF THERMODYNAMIC RELATIONS

Statistical mechanics formalism was used to determine thermodynamic properties of high T_C superconductors in the regime for the case of MgB₂. In the case of weak anisotropy, we extended the BCS model and showed the specific heat jump at T_C as compared to isotropic case as according to (Hensen, Mueller, Riek, & Scharnberg, 1997). The electron-phonon interactions between effective bands was measured with specific heat, leading to expression for variation of density of state and temperature, variation of order parameter and transition temperature, could be calculated.

This physics research was theoretical and expressions for quantities that lead to derived quantities were developed. Simplification of equation and generation of data calculations analyzed using Mathcad software for graphical tabulations and discussion.

The following approaches were adopted in achieving the objectives. Methodology was formulated with generalized description of the thermodynamics of two band superconductivity by taking into account impurity scattering for magnetic and nonmagnetic properties. The research took the model of two-band approach by combining the H_p, H_d, and H_{pd} whose results were applied to

MgB₂ using the first principles band-structure for the electron phonon interactions using quantum field theory to study effective attractive interactions between electrons.

The definition of operators was done by incorporating a set of creation and annihilation operators, with each operator referring to a particular state in representing electrons and cooper pair in the d-band and p-band layers. Operating order values, average order values and quassi-particles associated with p- and d- bands respectively were developed.

3.3 APPROXIMATIONS AND ASSUMPTIONS

Using the electron pairing model, a model Hamiltonian for two band model was developed by assuming non-interacting normal electrons and non-interacting cooper pairs. The Hamiltonian was subjected to Meanfield approximation which studies the behavior of high dimensional random models, through approximating and averaging over degrees of freedom. This resulted to formation of averaged Hamiltonian that is superfluid and quadratic for two band MgB₂ superconductor. The averaged Hamiltonian was subjected to Bogoliubov-Valatin Transformation equations, which is original canonical linear transformation to get a quassiparticle Hamiltonian. Bogoliubov-Valatin transformations, transforms old operators to new operators from 1st quantisation to 2nd quantisation that obey the commutation rules and diagonalize it to new Hamiltonian.

Interaction energy was developed using the normalized wave function by performing bra-ket vacuum state operation, followed by factorization then normalization. The average energy was multiplied by the thermal activation factor to get the total energy of system of MgB₂. The thermal activation factor does not change energy value but only relates it with temperature. From the

energy expression, an expression for specific heat capacity, Sommerfeld coefficient, entropy, transition temperature and density of state with relation to temperature were developed.

The superconductivity thermal and magnetic properties for varying nonmagnetic inter-band scattering rates were calculated within the framework of two band model. It was found that, relations for thermodynamic potential on external trajectory corresponding to solutions of equations had the form of sum of contributions of σ - and π - band.

Secondly, a comparison was performed on the phenomenological two band model and applied Mathcad software program developed for the model to extract the gaps and the values from the results. Good agreement of the two-band model with data was realized for the temperature dependence for total energy, specific heat capacity, entropy, and Sommerfeld coefficient and transition temperature. A conclusion was made that the model approach can be taken as a handy tool to analyze thermodynamic properties of high T_C superconductivity.

A theoretical approach of thermodynamics of density of states for superconductors in two band models was developed. The developed model was used to get to objectives and define expression for thermodynamic properties of high T_C superconductors in two band model using electron-phonon interactions between effective band in two gap system. Numerical results for the density of states and various thermodynamic quantities as a function of inter-band impurity scattering rate were computed.

3.4 SOFTWARES USED.

The Mathcad 2000 Professional software was used in simplifications of equations derived and generation of data.

CHAPTER FOUR

THEORETICAL DERIVATIONS

4.1 Thermodynamic Properties of High T_C Superconductors.

In electron phonon interaction, quantum field theory is needed to outline conventional superconductors and induction of effective attractive interactions between electrons. Isotopic effect in conventional superconductors' works only if superconductivity is purely due to electrons, when that happens, the transition temperature T_C is considered independent on the mass of the nucleons. Experiments as according to (Onnes, 1911), show that the transition temperature T_C depends strongly on the mass of the nucleons present, which hints that superconductivity is related to lattice motions which are phonons. Electrons will attract other electrons via lattice distortions which is called phonon mediated attractions between electrons. Theoretically the attractions are induced when two electrons exchange a virtual phonon which can be shown rigorously in quantum field theory. Electrons are fermions and we cannot have more than one electron in a quantum state, hence we do not have condensate state for fermions which requires many particles to stay on the ground state. However, fermions can form Bose Einstein condensate (BEC) state but do not condensate, a pair of fermions is a composite boson which is condensate and the fermions pair is known as a Cooper pair whose theory of superconductivity is known as BCS theory that discusses repulsive interactions of electrons with charge.

The model Hamiltonian is in the conclusion of BCS theory in Fermi liquid that as long as there are some attractive interactions, the Fermi liquid state will become unstable below some T_C . The pairing mechanism in heavy Fermions is not yet established properly and this is one of the

challenges in condensed matter physics (Allan, 2013). Even the specific superconducting properties are not clearly known (Keisuke & Daisuke, 2012)

4.2 Defining Operators

We shall incorporate the entire set of creation and annihilation operators with each operator referring to a particular state. The following are representations for electrons and cooper pairs in d-band and p-band layers.

k: Block value, where $-k$ is defined to always have the opposite spin to k: ie if

$k = \uparrow$, then $-k = \downarrow$ and vice versa.

$C_{k\uparrow}^+$: Creation of d-band and p-band electron and cooper pair at state k with spin up.

$C_{-k\downarrow}^+$: Creation of d-band and p-band electron and cooper pair at state k with spin down.

$C_{k\uparrow}$: Annihilation of d-band and p-band electron and cooper pair at k state with spin up.

$C_{-k\downarrow}$: Annihilation of d-band and p-band electron and cooper pair at k state with spin down.

$C_k^+ C_{-k}^+$: Operator order value.

$\langle C_k^+ C_{-k}^+ \rangle$: Operator average order value.

$C_{d\uparrow}^+ C_{-d\downarrow}^+$: Quassi particle associated with d-bands.

$C_{p\uparrow}^+ C_{-p\downarrow}^+$: Quassi particle associated with p-band.

\uparrow : Fermi level spin up.

\downarrow : Fermi level spin down.

4.3 Model Hamiltonian for two band model isotope.

Using the electron pairing model, J, Bardeen, L.N Cooper, and J.R Schrieffer (BCS), developed two fluid models for superconductivity in 1957 earning them Nobel Prize in physics. The model

assumed non-interacting normal electrons, non-interacting cooper pairs and correctly predicted much of the experimental observations. We introduced two types of Bogoliubov quassi particles associated with the two p and d bands of the normal pairing mechanism in each of the two separate bands as well as inter-band pairing between cooper pairs formed in different bands. According to BCS theory, a system admits a precursor phase of cooper pair droplets that undergoes a phase locking transition at critical temperature. We Considered a canonical two band Hamiltonian that contain a Fermi surface of p and d bands for effective Hamiltonian, which is BCS reduced Hamiltonian whose formulation is described for our system of Magnesium Diboride. We defined operators C_k^+ as creation operator for single electron state, operator C_k as destruction operator for single electron state, V_{dd} and V_{pp} as pairing interaction, V_{pd} pairing interchange between the two bands p and d and ε_k as particle energy for attractive pairing strength. We also considered two types of quassi particles, $(C_{p\uparrow}C_{-p\downarrow}^+)$ and $C_{d\uparrow}C_{-d\downarrow}^+$ associated with the two p and d bands respectively. The normal phonon pairing mechanism in each of the two separate bands as well as inter-band pairing between cooper pairs was formed at different bands, giving effective Hamiltonian below as adopted by (Sethna, 2012).

$$H = H_d + H_p + H_{int} \quad (4.10)$$

Where H_d and H_p are the BCS effective Hamiltonian for the respective d and p bands and H_{int} denotes interactive energy between the p and d bands with combined form of inter-band interaction.

$$H_d = \sum_{ks} \varepsilon_{ds} C_{k\sigma}^+ C_{k\sigma} + C_{-k\sigma}^+ C_{-k\sigma} - \sum_{k,k'} V_{dk^1k} C_{k\uparrow}^+ C_{-k\downarrow}^+ C_{k\uparrow} C_{-k^1\downarrow} + \sum_{kk^1} V_{dkk^1} C_{k\uparrow}^+ C_{-k\downarrow}^+ C_{k^1\uparrow} C_{-k^1\downarrow} \quad (4.11)$$

$$H_p = \sum_{ks} \varepsilon_{p\sigma} C_{k\sigma}^+ C_{k\sigma} + C_{-k\sigma}^+ C_{-k\sigma} - \sum_{kk^1} V_{pk^1k} C_{k\uparrow}^+ C_{-k\downarrow}^+ C_{k\uparrow} C_{-k\downarrow} + C_{-k^1\downarrow} C_{k\uparrow} \quad (4.12)$$

H_d denotes free electron and interaction energy in d band, H_p denotes the free electron and interaction energy in p band

Where the first term in equation (4.11) denotes energy of free electrons in d-band, second term denotes the interaction energy of cooper pairs in same layer in d-band of MgB₂, the third term denotes the energy of free electrons in d-band, while equation (4.12) first term denotes energy of free electrons in p-band, second term denotes the interaction energy of cooper pairs in same layer in p-band of MgB₂, the third term denotes the energy of free electrons in p-band.

In the present work, according to (Bogoliubov, 1947) Bogoliubov-Valatin has been used as mathematical tool for investigation of superconducting transition temperature, density of state, electronic specific heat and order parameter taking interlayer interaction between MgB₂. In equation (4.11) and (4.12), ε_{ds} and ε_{ps} are the kinetic energies of p and d bands, measured to relative Fermi level with spin (s) (\uparrow or \downarrow), where k is the block value and V_{pkk^1} and V_{dkk^1} are the inter-band phonon mediated interaction matrices respectively.

$$H_{hint} = -\sum_{k,k^1} V_{dpkk^1} (C_{k\uparrow}^+ C_{-k\downarrow}^+ C_{-k^1\downarrow} C_{k^1\uparrow} + C_{-k^1\downarrow} C_{k^1\uparrow} C_{k\uparrow}^+ C_{-k\downarrow}^+) \quad (4.13).$$

H_{hint} denote the interaction between the p and d bands and is the combined form for inter-band interaction with phonon mediated matrix element V_{dpk} .

This interaction is part of the electron interaction, here; we have ignored all other types of interaction. This turns out to be a good approximation because this interaction is the key which induces the pairs while all other interactions have effective energies, i.e hopping effective energies.

4.4 Mean Field Approximation

In BEC, we introduce order parameter $\langle C^+ \rangle$, where the pair of electrons forms the BEC state, so

that the order parameter can be written as $\sum_k \langle C_{k\uparrow}^+ C_{-k\downarrow}^+ \rangle$ where condensed phase $\langle C_{k\uparrow}^+ C_{-k\downarrow}^+ \rangle \neq 0$

$$C_{k\uparrow}^+ C_{-k\downarrow}^+ = \langle C_{k\uparrow}^+ C_{-k\downarrow}^+ \rangle + (C_{k\uparrow}^+ C_{-k\downarrow}^+ - \langle C_{k\uparrow}^+ C_{-k\downarrow}^+ \rangle) \quad (4.14)$$

hence;

$$C_{k^1\uparrow} C_{-k^1\downarrow} = \langle C_{k^1\uparrow} C_{-k^1\downarrow} \rangle + (C_{k^1\uparrow} C_{-k^1\downarrow} - \langle C_{k^1\uparrow} C_{-k^1\downarrow} \rangle) \quad (4.15)$$

The physical meaning of equation (4.14) is the operator $C_{k\uparrow}^+ C_{-k\downarrow}^+$ with average value $\langle C_{k\uparrow}^+ C_{-k\downarrow}^+ \rangle$ and

operator fluctuates around this average value with fluctuations being $(C_{k\uparrow}^+ C_{-k\downarrow}^+ - \langle C_{k\uparrow}^+ C_{-k\downarrow}^+ \rangle)$. The

same operation happens to equation (4.15). We let the fluctuations of the operator be small, the

last term in the formulas becomes small. We now defined X_{pd} and X_{pd}^+ as

$$\langle C_{k\uparrow}^+ C_{-k\downarrow}^+ \rangle = X_{pd}^+ \quad (4.16)$$

$$\langle C_{k\uparrow} C_{-k\downarrow} \rangle = X_{pd} \quad (4.17)$$

respectively and we let equation (4.16) and (4.17) be used to define and formulate the fluctuation

term as below,

$$\sum_{k,k^1} V_{dkk^1} X_{pd}^+ \cdot X_{pd} = \sum_{kk^1} V_{pdkk^1} (X_{pd}^+ + (X_{pd}^+ - X_{pd}^*)) (X_{pd}^+ + (C_{k^1\downarrow} C_{k^1\uparrow} - X_{pd})) \quad (4.18)$$

The fluctuation term was generated by substituting equations (4.14), (4.15), (4.16) and (4.17)

into equation (4.18) to get equation (4.19).

$$\begin{aligned} H_{Fluctuation} &= \sum_{k,k^1} V_{pdkk^1} C_{k\uparrow}^+ C_{-k\downarrow}^+ C_{k^1\downarrow} C_{-k^1\uparrow} = \sum_{kk^1} V_{pdkk^1} (X_{pd}^+ + (C_{k\uparrow}^+ C_{-k\downarrow}^+ - X_{pd}^*)) (X_{pd}^+ + (C_{k^1\downarrow} C_{-k^1\uparrow} - X_{pd})) \\ &= V_{pdkk^1} [X_{pd}^+ X_{pd} + X_{pd}] (C_{k^1\downarrow} C_{-k^1\uparrow} - X_{pd}) + (C_{k\uparrow}^+ C_{-k\downarrow}^+ - X_{pd}^+) + \text{very - small - factor} \end{aligned} \quad (4.19)$$

We write the interaction terms of the values X_{pd} and X_{pd}^+ as fluctuations

the last term of equation (4.19) $V \sum_{kk^1} [(C_{k^1\uparrow}^+ C_{-k\downarrow}^+ - X_k^+) (C_{k^1\uparrow} C_{-k^1\downarrow} - X_{k^1})]$ is fluctuations times

fluctuations, hence the last part is smallest hence ignored.

We introduced gap parameters for p and d bands respectively.

$$\Delta_{dd}^+ = V_{dk} \sum_k X_d^* = V_{dkk^1} \langle C_{k^1\uparrow}^+ C_{-k\downarrow}^+ \rangle \quad (4.20)$$

$$\Delta_{dd} = C_{k^1\downarrow} C_{-k\uparrow} + V_{dd} C_{k^1\uparrow}^+ C_{-k\downarrow}^+ \quad (4.21)$$

$$\Delta_{pp}^+ = V_{ppk^1} \sum_k X_k \quad (4.22)$$

$$\Delta_{pp} = V_{pkk^1} \sum_k X_p \quad (4.23)$$

Hence equation (4.11) and (4.12) are subjected to fluctuation term in equation (4.19) and gap

parameters in equation (4.20),(4.21) and (4.22) to get equation (4.24) and (4.25)

$$H_d = \sum_{ks} \varepsilon_{ds} \left(C_{k^1\uparrow}^+ C_{k\uparrow} + \Delta_{dd}^+ \sum_{k^1} C_{k^1\downarrow} C_{-k\uparrow} + \Delta_{dd} C_{k^1\uparrow}^+ C_{-k\downarrow}^+ \right) \quad (4.24)$$

Similarly weredefined equation (4.12) to get equation (4.25)

hence

$$H_p = \varepsilon_{ks} (C_{ks}^+ C_{ks} + C_{-ks}^+ C_{-ks}) + \Delta_{pp}^+ \sum_k C_{k^1\downarrow} C_{-k\uparrow} + \Delta_{pp} \sum_k C_{k\downarrow}^+ C_{k^1\downarrow} \quad (4.25)$$

Then the Hamiltonian of the two band system reduces to

$$H_o^p = V_{ppk^1\uparrow} \sum_p \varepsilon_p \mu (C_{p^1\uparrow}^+ C_{p\uparrow} + C_{-p\downarrow}^+ C_{-p\downarrow}) + \Delta_{pp}^+ \sum_p C_{-p\downarrow} C_{p\uparrow} + \Delta_{pp} \sum_p C_{p^1\uparrow}^+ C_{-p\downarrow} \quad (4.26)$$

$$H_o^d = V_{ddk^1\uparrow} \sum_d \varepsilon_d \mu (C_{d^1\uparrow}^+ C_{d\uparrow} + C_{-d\downarrow}^+ C_{-d\downarrow}) + \Delta_{dd}^+ \sum_d C_{-d\downarrow} C_{d\uparrow} + \Delta_{dd} \sum_d C_{d^1\uparrow}^+ C_{-d\downarrow} \quad (4.27)$$

$$H_{hint} = - \sum_{k,k^1} V_{dpkk^1} (C_{k^1\uparrow}^+ C_{-k\downarrow}^+ C_{-k^1\downarrow} C_{k^1\uparrow} + C_{-k^1\downarrow} C_{k^1\uparrow} C_{k^1\uparrow}^+ C_{-k\downarrow}^+) \quad (4.28)$$

Where p and d are momentum labels in the d - and p -bands respectively with energies

ϵ_p and ϵ_d , μ is the common chemical potential. Each band has its proper pairing interaction V_{pp} and V_{dd} , while the pair interchange between the two bands is assured by V_{pd} term.

We have assumed $V_{pd}=V_{dp}$ and we redefined equation (4.13) as H_{pd}

$$H_{pd} = \Delta_1^+ \sum_d C_{-d\downarrow} C_{d\uparrow} + \Delta_2 \sum_p C_{-p\downarrow}^+ C_{p\uparrow}^+ + \Delta_2^+ \sum_p C_{-p\downarrow} C_{p\uparrow} + \Delta_1 \sum_d C_{d\uparrow}^+ C_{-d\downarrow}^+ \quad (4.29)$$

Final Hamiltonian is a superfluid quadratic Hamiltonian, which is summation for equations (4.27), (4.28) and (4.29).

$$\begin{aligned} H = & V_{ppk\uparrow} \sum_p \epsilon_p u \left(C_{p\uparrow}^+ C_{p\uparrow} + C_{-p\downarrow}^+ C_{-p\downarrow} \right) + \Delta_{pp}^+ \sum_p C_{-p\downarrow} C_{p\uparrow} + \Delta_{pp} \sum_p C_{p\uparrow}^+ C_{-p\downarrow}^+ \\ & + V_{ddk\uparrow} \sum_d \epsilon_d u \left(C_{d\uparrow}^+ C_{d\uparrow} + C_{-d\downarrow}^+ C_{-d\downarrow} \right) + \Delta_{dd}^+ \sum_d C_{-d\downarrow} C_{d\uparrow} + \Delta_{dd} \sum_d C_{d\uparrow}^+ C_{-d\downarrow}^+ \\ & + \Delta_1^+ \sum_d C_{-d\downarrow} C_{d\uparrow} + \Delta_2 \sum_p C_{-p\downarrow}^+ C_{p\uparrow}^+ + \Delta_2^+ \sum_p C_{-p\downarrow} C_{p\uparrow} + \Delta_1 \sum_d C_{d\uparrow}^+ C_{-d\downarrow}^+ \end{aligned} \quad (4.30)$$

4.5 Bogoliubov-Valatin Transformations

Is the original Canonical linear transformations to diagonalise quadratic Hamiltonian in superfluid was introduced by (Bogoliubov, 1947), and later extended by both Bogoliubov and Valatin, (Valatin, 1958) and (Bogoliubov & Valatin, 1958) to theory of Fermi surface in superconductivity. The applications of BV transformations were done to both bosonic and fermionic versions in approximating BCS Hamiltonian in quadratic form and diagonalizing the results. In describing non interacting gas of quasi particles, BV transformations course is very standard in modern condensed matter physics where quadratic Hamiltonian can be solved exactly by basically studying the spectrum of the system of electrons. Bogoliubov-Valatin transformations, (Bogoliubov & Valatin, 1958) were introduced in variation principles for simplicity in reproducing results of the BCS theory of electron interaction with an easy extension to the case of electrons interacting with phonons, (Sergio *et al.*, (2008)).

Equation (4.31) is the adopted superfluid quadratic Hamiltonian for MgB₂ system which is diagonalized to obtain the elements of Hamiltonian that corresponds to stationary states when the system is in equilibrium by making use of the Bogoliubov-Valatin. We describe the superconducting states at T>0, we develop independently Bogoliubov and Valatin equations now known as Bogoliubov-Valatin Canonical transformation equations whose description is more appropriate as follows;

Since the model is dealing with large number of particles, the fluctuation about the average of

$\langle C_{-k\downarrow}^{\rightarrow} C_{k\uparrow}^{\rightarrow} \rangle$ would be small. We redefine C number operator as $C_{\vec{k}}^{\rightarrow}$ to conform to B.V status

$$C_{-k\downarrow}^{\rightarrow} C_{k\uparrow}^{\rightarrow} = C_{\vec{k}}^{+\rightarrow} + \left(C_{-k\downarrow}^{\rightarrow} C_{k\uparrow}^{\rightarrow} - C_{\vec{k}}^{+\rightarrow} \right) \quad (4.31)$$

Now for interaction term $\Delta_1^+ \sum_d C_{-d\downarrow} C_{d\uparrow} + \Delta_2 \sum_p C_{-p\downarrow}^+ C_{p\uparrow}^+ + \Delta_2^+ \sum_p C_{-p\downarrow} C_{p\uparrow} + \Delta_1 \sum_d C_{d\uparrow}^+ C_{-d\downarrow}^+$ in

equation (4.30), we substitute equation (4.32) into equation (4.30) to get equation (4.33)

$$\begin{aligned} H_{pd} &= \sum_{\vec{k}\sigma} V_{\vec{k}} C_{\vec{k}\uparrow}^+ C_{\vec{k}\uparrow}^+ C_{-\vec{k}\downarrow} C_{-\vec{k}\downarrow} = \sum_{\vec{k}} V_{\vec{k}} \left(C_{\vec{k}} + \begin{pmatrix} C_{\vec{k}\uparrow}^+ & C_{\vec{k}\uparrow}^+ & -C_{\vec{k}} \end{pmatrix} \right) \left(C_{\vec{k}} + \begin{pmatrix} C_{-\vec{k}\downarrow} & C_{\vec{k}\uparrow} & -C_{\vec{k}} \end{pmatrix} \right) \\ &= \sum_{\vec{k}} V_{\vec{k}} \left[C_{\vec{k}} C_{\vec{k}}^+ C_{\vec{k}}^+ - C_{\vec{k}}^+ C_{\vec{k}} + C_{\vec{k}} C_{-\vec{k}\downarrow} C_{-\vec{k}\downarrow} + \begin{pmatrix} C_{\vec{k}\uparrow}^+ & C_{\vec{k}\uparrow}^+ & -C_{\vec{k}} \end{pmatrix} \begin{pmatrix} C_{-\vec{k}\downarrow} & C_{\vec{k}\uparrow} & -C_{\vec{k}} \end{pmatrix} \right] \end{aligned} \quad (4.32)$$

We ignored the last term on the right hand side of equation (4.33) because it's small due to large number of particles therefore ignored.

$$\sum_{\vec{k}} V_{\vec{k}} C_{\vec{k}\uparrow}^+ C_{\vec{k}\uparrow}^+ C_{-\vec{k}\downarrow} C_{-\vec{k}\downarrow} = \sum_{\vec{k}} V_{\vec{k}} \left(C_{\vec{k}\uparrow}^+ C_{-\vec{k}\downarrow} C_{\vec{k}\uparrow} + C_{-\vec{k}\downarrow} C_{\vec{k}\uparrow}^+ C_{-\vec{k}\downarrow} - C_{\vec{k}\uparrow}^+ C_{\vec{k}\uparrow} \right) \quad (4.33)$$

Subject equation (4.34) to a constraint defined in equation (4.35)

$$u = \langle C_{-\vec{k}\downarrow} C_{\vec{k}\uparrow} \rangle_{average}. \quad (4.34)$$

We define the parameter

$$\Delta_{\vec{k}} = \sum_{\vec{k}} V_{\vec{k}} u = - \sum_{\vec{k}} V_{\vec{k}}^+ \langle C_{-\vec{k}\downarrow} C_{\vec{k}\uparrow} \rangle \quad (4.35)$$

Lead

$$H_{pd} = +\Delta_1^+ \sum_d C_{-d\downarrow} C_{d\uparrow} + \Delta_2 \sum_p C_{-p\downarrow}^+ C_{p\uparrow}^+ + \Delta_2^+ \sum_p C_{-p\downarrow} C_{p\uparrow} + \left(C_{-\vec{k}\downarrow} C_{\vec{k}\uparrow} - C_{\vec{k}\uparrow}^+ \right) + \sum_d C_{d\uparrow}^+ C_{-d\downarrow}^+ \quad (4.36)$$

The same operation is done on second part of equation (4.31), for H_d by substituting equation

(4.32) to get

$$H_d = \sum_d \epsilon_d \left(C_{d\uparrow}^+ C_{d\uparrow} + C_{-d\downarrow}^+ C_{-d\downarrow} \right) + \Delta_{dd}^+ \sum_d C_{\vec{k}}^+ + \left(C_{-\vec{k}\downarrow} C_{\vec{k}\uparrow} - C_{\vec{k}\downarrow}^+ \right) + \Delta_{dd} \sum_d C_{d\uparrow}^+ C_{-d\downarrow}^+ \quad (4.37)$$

Lastly the same operation of substituting of equation (4.32) into the first part of equation (4.30)

for H_p

$$H_p = \sum_p \epsilon_p \left(C_{p\uparrow}^+ C_{p\uparrow} + C_{-p\downarrow}^+ C_{-p\downarrow} \right) + \Delta_{pp}^+ \sum_p C_{-k\downarrow}^+ + \left(C_{-k\downarrow}^+ C_{k\uparrow}^+ - C_{k\uparrow}^+ \right) + \Delta_{pp} \sum_p C_{p\uparrow}^+ C_{-p\downarrow}^+ \quad (4.38)$$

The total Hamiltonian after the above operations becomes bilinear form, hence diagonalisable.

$$\begin{aligned} H &= \sum_p \epsilon_p \left(C_{p\uparrow}^+ C_{p\uparrow} + C_{-p\downarrow}^+ C_{-p\downarrow} \right) + \Delta_{pp}^+ \sum_p C_{-k\downarrow}^+ + \left(C_{-k\downarrow}^+ C_{k\uparrow}^+ - C_{k\uparrow}^+ \right) + \Delta_{pp} \sum_p C_{p\uparrow}^+ C_{-p\downarrow}^+ \\ &+ \sum_d \epsilon_d \left(C_{d\uparrow}^+ C_{d\uparrow} + C_{-d\downarrow}^+ C_{-d\downarrow} \right) + \Delta_{dd}^+ \sum_d C_{-k\downarrow}^+ + \left(C_{-k\downarrow}^+ C_{k\uparrow}^+ - C_{k\uparrow}^+ \right) + \Delta_{dd} \sum_d C_{d\uparrow}^+ C_{-d\downarrow}^+ \\ &+ \Delta_1^+ \sum_d C_{-d\downarrow}^+ C_{d\uparrow} + \Delta_2 \sum_p C_{-p\downarrow}^+ C_{p\uparrow} + \Delta_2^+ \sum_p C_{-k\downarrow}^+ + \left(C_{-k\downarrow}^+ C_{k\uparrow}^+ - C_{k\uparrow}^+ \right) + \sum_d C_{d\uparrow}^+ C_{-d\downarrow}^+ \end{aligned} \quad (4.39)$$

Noting that the operators in equation (4.40) appear in bilinear form, they can be written in a diagonal form by appropriate transformations using C operators as shown in Bogoliubov and Valatin. We define C operators to B.V terms as in equation (4.41).

$$\begin{aligned} C_{\rightarrow k} &= u_{\rightarrow k}^+ \gamma_{\rightarrow k} + v_{\rightarrow k} \gamma_{\rightarrow k}^+ \\ C_{\rightarrow k}^+ &= -v_{\rightarrow k}^+ \gamma_{\rightarrow k} + u_{\rightarrow k} \gamma_{\rightarrow k}^+ \end{aligned} \quad (4.40)$$

Where γ satisfy the following commutation rules

$$\left[\gamma_{\rightarrow k}^+, \gamma_{\rightarrow k} \right]_+ = \delta_{\rightarrow kk} \quad (4.41)$$

$$\gamma_{\rightarrow k}^+ \gamma_{\rightarrow k}^+ = \gamma_{\rightarrow k} \gamma_{\rightarrow k} = 0 \quad (4.42)$$

We can also note that $u_{\rightarrow k}$ and $v_{\rightarrow k}$ satisfy

$$\left[\frac{u_{\rightarrow k}}{k} \right]^2 + \left[\frac{v_{\rightarrow k}}{k} \right]^2 = 1 \quad (4.43)$$

We also defined quassi particles $C_{\vec{k}}^+ C_{\vec{k}}$, $C_{-\vec{k}}^+ C_{-\vec{k}}$, $C_{\vec{k}}^+ C_{-\vec{k}}^+$ and $C_{-\vec{k}} C_{\vec{k}}$ separately to conform

to B.V diagonalised expression as bellow according to Bogoliubov and Valatin, (1969)

$$\begin{aligned}
C_{\vec{k}}^+ C_{\vec{k}} &= \left(u_{\vec{k}} \gamma_{\vec{k}}^+ + u_{\vec{k}}^+ \gamma_{\vec{k}} \right) \left(u_{\vec{k}}^+ \gamma_{\vec{k}} + u_{\vec{k}} \gamma_{\vec{k}}^+ \right) \\
&= \left| u_{\vec{k}} \right|^2 \gamma_{\vec{k}}^+ \gamma_{\vec{k}} + u_{\vec{k}}^+ v_{\vec{k}}^+ \gamma_{\vec{k}} \gamma_{\vec{k}} + u_{\vec{k}} \gamma_{\vec{k}} \gamma_{\vec{k}} \gamma_{\vec{k}} + \left| u_{\vec{k}}^+ \right|^2 \gamma_{\vec{k}} \gamma_{\vec{k}}^+.
\end{aligned} \tag{4.44}$$

$$\begin{aligned}
C_{-\vec{k}}^+ C_{-\vec{k}} &= \left(-v_{\vec{k}}^+ \gamma_{\vec{k}} + u_{\vec{k}} \gamma_{\vec{k}} \right) \left(-v_{\vec{k}} \gamma_{\vec{k}}^+ + u_{\vec{k}}^+ \gamma_{\vec{k}}^+ \right) \\
&= \left| v_{\vec{k}} \right|^2 \gamma_{\vec{k}}^+ \gamma_{\vec{k}}^+ - u_{\vec{k}} v_{\vec{k}}^+ \gamma_{\vec{k}}^+ \gamma_{\vec{k}} - u_{\vec{k}}^+ v_{\vec{k}} \gamma_{\vec{k}} \gamma_{\vec{k}}^+ + \left| v_{\vec{k}}^+ \right|^2 \gamma_{\vec{k}} \gamma_{\vec{k}}.
\end{aligned} \tag{4.45}$$

Similarly

$$\begin{aligned}
C_{\vec{k}}^+ C_{-\vec{k}}^+ &= \left(u_{\vec{k}} \gamma_{\vec{k}}^+ + u_{\vec{k}}^+ \gamma_{\vec{k}} \right) \left(-v_{\vec{k}}^+ \gamma_{\vec{k}} + u_{\vec{k}} \gamma_{\vec{k}} \right) = u_{\vec{k}} v_{\vec{k}}^+ \gamma_{\vec{k}}^+ \gamma_{\vec{k}} \\
&- \left| v_{\vec{k}} \right|^2 \gamma_{\vec{k}} \gamma_{\vec{k}} + u_{\vec{k}}^2 \gamma_{\vec{k}}^+ \gamma_{\vec{k}}^+ + u_{\vec{k}}^+ v_{\vec{k}} \gamma_{\vec{k}} \gamma_{\vec{k}}^+.
\end{aligned} \tag{4.46}$$

$$\begin{aligned}
C_{-\vec{k}} C_{\vec{k}} &= \left(-v_{\vec{k}} \gamma_{\vec{k}}^+ + u_{\vec{k}}^+ \gamma_{\vec{k}}^+ \right) \left(u_{\vec{k}}^+ \gamma_{\vec{k}} + v_{\vec{k}} \gamma_{\vec{k}} \right) = -v_{\vec{k}}^+ u_{\vec{k}}^+ \gamma_{\vec{k}}^+ \gamma_{\vec{k}} \\
&+ \left| u_{\vec{k}} \right|^2 \gamma_{\vec{k}} \gamma_{\vec{k}} - \left| v_{\vec{k}} \right|^2 \gamma_{\vec{k}}^+ \gamma_{\vec{k}}^+ + u_{\vec{k}}^+ v_{\vec{k}} \gamma_{\vec{k}} \gamma_{\vec{k}}^+.
\end{aligned} \tag{4.47}$$

We now substitute these values in equations, (4.41), (4.45),(4.46),(4.47) and (4.48) into equation (4.38) of the Hamiltonian, considering the first term we have to get equation (4.49)

$$\begin{aligned}
H_d = & \in_d \left(\left| \mathbf{u}_{\vec{k}} \right|^2 \gamma_{\vec{k}}^+ \gamma_{\vec{k}} + \mathbf{u}_{\vec{k}}^+ \mathbf{v}_{\vec{k}}^+ \gamma_{\vec{k}} \gamma_{-\vec{k}} + \mathbf{u}_{\vec{k}} \mathbf{v}_{\vec{k}} \gamma_{\vec{k}} \gamma_{-\vec{k}} + \left| \mathbf{v}_{\vec{k}}^+ \right|^2 \gamma_{\vec{k}} \gamma_{-\vec{k}}^+ \right) \\
& + \Delta_{dd}^+ \sum_d \gamma_{\vec{k}}^+ + \left(-\mathbf{v}_{\vec{k}}^+ \mathbf{u}_{\vec{k}}^+ \gamma_{\vec{k}}^+ \gamma_{-\vec{k}} + \left| \mathbf{u}_{\vec{k}} \right|^2 \gamma_{\vec{k}} \gamma_{-\vec{k}} - \left| \mathbf{v}_{\vec{k}} \right|^2 \gamma_{\vec{k}}^+ \gamma_{-\vec{k}}^+ + \mathbf{u}_{\vec{k}}^+ \mathbf{v}_{\vec{k}} \gamma_{\vec{k}} \gamma_{-\vec{k}} \gamma_{\vec{k}}^+ + \mathbf{v}_{\vec{k}}^+ \gamma_{\vec{k}} + \mathbf{u}_{\vec{k}} \gamma_{\vec{k}}^+ \right) + \\
& \Delta_{dd} \sum_d \mathbf{u}_{\vec{k}} \mathbf{v}_{\vec{k}}^+ \gamma_{\vec{k}}^+ - \left| \mathbf{v}_{\vec{k}} \right|^2 \gamma_{\vec{k}} \gamma_{-\vec{k}} + \mathbf{u}_{\vec{k}}^2 \gamma_{\vec{k}}^+ \gamma_{-\vec{k}}^+ + \mathbf{u}_{\vec{k}}^+ \mathbf{v}_{\vec{k}} \gamma_{\vec{k}} \gamma_{-\vec{k}}^+. \tag{4.48}
\end{aligned}$$

When the coefficients of $\gamma_{\vec{k}} \gamma_{-\vec{k}}$ and $\gamma_{\vec{k}}^+ \gamma_{-\vec{k}}^+$ vanish in the terms, equation (4.49) is diagonalised

to give equation (4.50)

$$\begin{aligned}
H_d = & \in_d \left(\left| \mathbf{u}_{\vec{k}} \right|^2 \gamma_{\vec{k}}^+ \gamma_{-\vec{k}} + \gamma_{\vec{k}} \gamma_{\vec{k}} + \gamma_{\vec{k}} \gamma_{-\vec{k}} + \left| \mathbf{v}_{\vec{k}}^+ \right|^2 \gamma_{\vec{k}} \gamma_{-\vec{k}}^+ + \gamma_{\vec{k}}^+ \gamma_{-\vec{k}}^+ - \mathbf{u}_{\vec{k}} \mathbf{v}_{\vec{k}} \gamma_{\vec{k}} - \gamma_{\vec{k}} \gamma_{-\vec{k}} + \left| \mathbf{v}_{\vec{k}}^+ \right|^2 \gamma_{\vec{k}}^+ \gamma_{-\vec{k}} \right) \\
& + \Delta_{dd}^+ \sum_d \gamma_{\vec{k}}^+ + \left(-\mathbf{v}_{\vec{k}}^+ \mathbf{u}_{\vec{k}}^+ \gamma_{\vec{k}}^+ \gamma_{-\vec{k}} + \gamma_{\vec{k}} \gamma_{\vec{k}} - \gamma_{\vec{k}}^+ \gamma_{-\vec{k}}^+ + \mathbf{u}_{\vec{k}}^+ \mathbf{v}_{\vec{k}} \gamma_{\vec{k}} \gamma_{-\vec{k}} \gamma_{\vec{k}}^+ + \mathbf{v}_{\vec{k}}^+ \gamma_{\vec{k}} + \mathbf{u}_{\vec{k}} \gamma_{\vec{k}}^+ \right) + \\
& \Delta_{dd} \sum_d \mathbf{u}_{\vec{k}} \mathbf{v}_{\vec{k}}^+ \gamma_{\vec{k}}^+ - \gamma_{\vec{k}} \gamma_{\vec{k}} + \gamma_{\vec{k}}^+ \gamma_{-\vec{k}}^+ + \mathbf{u}_{\vec{k}}^+ \mathbf{v}_{\vec{k}} \gamma_{\vec{k}} \gamma_{-\vec{k}}^+. \tag{4.49}
\end{aligned}$$

Collecting like terms, equation (4.50) becomes equation (4.51)

$$\begin{aligned}
H_d = & \in_d \left(\left| \mathbf{u}_{\vec{k}} \right|^2 \gamma_{\vec{k}}^+ \gamma_{-\vec{k}} + \gamma_{\vec{k}} \gamma_{\vec{k}} + \left| \mathbf{v}_{\vec{k}}^+ \right|^2 \gamma_{\vec{k}} \gamma_{-\vec{k}}^+ + \gamma_{\vec{k}}^+ \gamma_{-\vec{k}}^+ - \mathbf{u}_{\vec{k}} \mathbf{v}_{\vec{k}} \gamma_{\vec{k}} + \left| \mathbf{v}_{\vec{k}}^+ \right|^2 \gamma_{\vec{k}}^+ \gamma_{-\vec{k}} \right) \\
& + \Delta_{dd}^+ \sum_d \gamma_{\vec{k}}^+ + \left(-\mathbf{v}_{\vec{k}}^+ \mathbf{u}_{\vec{k}}^+ \gamma_{\vec{k}}^+ \gamma_{-\vec{k}} + \gamma_{\vec{k}} \gamma_{\vec{k}} - \gamma_{\vec{k}}^+ \gamma_{-\vec{k}}^+ + \mathbf{u}_{\vec{k}}^+ \mathbf{v}_{\vec{k}} \gamma_{\vec{k}} \gamma_{-\vec{k}} \gamma_{\vec{k}}^+ + \mathbf{v}_{\vec{k}}^+ \gamma_{\vec{k}} + \mathbf{u}_{\vec{k}} \gamma_{\vec{k}}^+ \right) + \\
& \Delta_{dd} \sum_d \mathbf{u}_{\vec{k}} \mathbf{v}_{\vec{k}}^+ \gamma_{\vec{k}}^+ - \gamma_{\vec{k}} \gamma_{-\vec{k}} + \gamma_{\vec{k}}^+ \gamma_{\vec{k}}^+ + \mathbf{u}_{\vec{k}}^+ \mathbf{v}_{\vec{k}} \gamma_{\vec{k}} \gamma_{-\vec{k}}^+. \tag{4.50}
\end{aligned}$$

We now substitute these values in equations (4.41), (4.45),(4.46),(4.47) and (4.48) into equation (4.39) of the Hamiltonian, considering the first term we get equation (4.52)

$$\begin{aligned}
H_p = & \epsilon_p \sum_p \left(\left| \mathbf{u}_{\vec{k}} \right|^2 \gamma_{\vec{k}}^+ \gamma_{\vec{k}} + \mathbf{u}_{\vec{k}}^+ \mathbf{v}_{\vec{k}}^+ \gamma_{\vec{k}} \gamma_{\vec{k}} + \mathbf{u}_{\vec{k}} \mathbf{v}_{\vec{k}} \gamma_{\vec{k}} \gamma_{\vec{k}} + \right. \\
& \left. \left| \mathbf{v}_{\vec{k}}^+ \right|^2 \gamma_{\vec{k}} \gamma_{\vec{k}}^+ + \left| \mathbf{v}_{\vec{k}} \right|^2 \gamma_{\vec{k}}^+ \gamma_{\vec{k}} - \mathbf{u}_{\vec{k}} \mathbf{v}_{\vec{k}} \gamma_{\vec{k}} - \mathbf{u}_{\vec{k}}^+ \mathbf{v}_{\vec{k}}^+ \gamma_{\vec{k}} \gamma_{\vec{k}} + \left| \mathbf{v}_{\vec{k}}^+ \right|^2 \gamma_{\vec{k}}^+ \gamma_{\vec{k}} \right) \\
& + \Delta_{pp}^+ \sum_p \gamma_{\vec{k}}^+ + \left(-\mathbf{v}_{\vec{k}}^+ \mathbf{u}_{\vec{k}}^+ \gamma_{\vec{k}}^+ \gamma_{\vec{k}} + \left| \mathbf{u}_{\vec{k}} \right|^2 \gamma_{\vec{k}} \gamma_{\vec{k}} - \left| \mathbf{v}_{\vec{k}} \right|^2 \gamma_{\vec{k}}^+ \gamma_{\vec{k}}^+ + \mathbf{u}_{\vec{k}}^+ \mathbf{v}_{\vec{k}} \gamma_{\vec{k}} \gamma_{\vec{k}} \gamma_{\vec{k}}^+ + \mathbf{v}_{\vec{k}}^+ \gamma_{\vec{k}} + \mathbf{u}_{\vec{k}} \gamma_{\vec{k}}^+ \right) + \\
& \Delta_{pp} \sum_d \mathbf{u}_{\vec{k}} \mathbf{v}_{\vec{k}}^+ \gamma_{\vec{k}}^+ - \left| \mathbf{v}_{\vec{k}} \right|^2 \gamma_{\vec{k}} \gamma_{\vec{k}} + \mathbf{u}_{\vec{k}}^2 \gamma_{\vec{k}}^+ \gamma_{\vec{k}}^+ + \mathbf{u}_{\vec{k}}^+ \mathbf{v}_{\vec{k}} \gamma_{\vec{k}} \gamma_{\vec{k}}^+. \tag{4.51}
\end{aligned}$$

When the coefficients of $\gamma_{\vec{k}} \gamma_{\vec{k}}$ and $\gamma_{\vec{k}}^+ \gamma_{\vec{k}}^+$ vanish in the terms, equation (4.51) is diagonalised

to give equation (4.52)

$$\begin{aligned}
H_p = & \epsilon_p \sum_p \left(\left| \mathbf{u}_{\vec{k}} \right|^2 \gamma_{\vec{k}}^+ \gamma_{\vec{k}} + \gamma_{\vec{k}} \gamma_{\vec{k}} + \gamma_{\vec{k}} \gamma_{\vec{k}} + \left| \mathbf{v}_{\vec{k}}^+ \right|^2 \gamma_{\vec{k}} \gamma_{\vec{k}}^+ + \gamma_{\vec{k}}^+ \gamma_{\vec{k}}^+ - \mathbf{u}_{\vec{k}} \mathbf{v}_{\vec{k}} \gamma_{\vec{k}} - \gamma_{\vec{k}} \gamma_{\vec{k}} + \left| \mathbf{v}_{\vec{k}}^+ \right|^2 \gamma_{\vec{k}}^+ \gamma_{\vec{k}} \right) \\
& + \Delta_{pp}^+ \sum_p \gamma_{\vec{k}}^+ + \left(-\mathbf{v}_{\vec{k}}^+ \mathbf{u}_{\vec{k}}^+ \gamma_{\vec{k}}^+ \gamma_{\vec{k}} + \gamma_{\vec{k}} \gamma_{\vec{k}} - \gamma_{\vec{k}}^+ \gamma_{\vec{k}}^+ + \mathbf{u}_{\vec{k}}^+ \mathbf{v}_{\vec{k}} \gamma_{\vec{k}} \gamma_{\vec{k}} \gamma_{\vec{k}}^+ + \mathbf{v}_{\vec{k}}^+ \gamma_{\vec{k}} + \mathbf{u}_{\vec{k}} \gamma_{\vec{k}}^+ \right) + \\
& \Delta_{pp} \sum_d \mathbf{u}_{\vec{k}} \mathbf{v}_{\vec{k}}^+ \gamma_{\vec{k}}^+ - \gamma_{\vec{k}} \gamma_{\vec{k}} + \gamma_{\vec{k}}^+ \gamma_{\vec{k}}^+ + \mathbf{u}_{\vec{k}}^+ \mathbf{v}_{\vec{k}} \gamma_{\vec{k}} \gamma_{\vec{k}}^+. \tag{4.52}
\end{aligned}$$

Like terms were collected from equation (4.52) to give equation (4.53)

$$\begin{aligned}
H_p = & \epsilon_p \sum_p \left(\left| \mathbf{u}_{\vec{k}} \right|^2 \gamma_{\vec{k}}^+ \gamma_{\vec{k}} + \gamma_{\vec{k}} \gamma_{\vec{k}} + \left| \mathbf{v}_{\vec{k}}^+ \right|^2 \gamma_{\vec{k}} \gamma_{\vec{k}}^+ + \gamma_{\vec{k}}^+ \gamma_{\vec{k}}^+ - \mathbf{u}_{\vec{k}} \mathbf{v}_{\vec{k}} \gamma_{\vec{k}} + \left| \mathbf{v}_{\vec{k}}^+ \right|^2 \gamma_{\vec{k}}^+ \gamma_{\vec{k}} \right) \\
& + \Delta_{pp}^+ \sum_p \gamma_{\vec{k}}^+ + \left(-\mathbf{v}_{\vec{k}}^+ \mathbf{u}_{\vec{k}}^+ \gamma_{\vec{k}}^+ \gamma_{\vec{k}} + \gamma_{\vec{k}} \gamma_{\vec{k}} - \gamma_{\vec{k}}^+ \gamma_{\vec{k}}^+ + \mathbf{u}_{\vec{k}}^+ \mathbf{v}_{\vec{k}} \gamma_{\vec{k}} \gamma_{\vec{k}} \gamma_{\vec{k}}^+ + \mathbf{v}_{\vec{k}}^+ \gamma_{\vec{k}} + \mathbf{u}_{\vec{k}} \gamma_{\vec{k}}^+ \right) + \\
& \Delta_{pp} \sum_d \mathbf{u}_{\vec{k}} \mathbf{v}_{\vec{k}}^+ \gamma_{\vec{k}}^+ - \gamma_{\vec{k}} \gamma_{\vec{k}} + \gamma_{\vec{k}}^+ \gamma_{\vec{k}}^+ + \mathbf{u}_{\vec{k}}^+ \mathbf{v}_{\vec{k}} \gamma_{\vec{k}} \gamma_{\vec{k}}^+. \tag{4.53}
\end{aligned}$$

We now substitute values in equations (4.40), (4.44), (4.45), (4.46) and (4.47) into equation (4.36)

of the Hamiltonian, considering the first term we have to get equation (4.54)

$$\begin{aligned}
H_{pd} = & \Delta_1^+ \sum_d \left(-v_{\vec{k}}^+ u_{\vec{k}}^+ \gamma_{\vec{k}}^+ \gamma_{-\vec{k}} + \left| u_{\vec{k}} \right|^2 \gamma_{\vec{k}} \gamma_{-\vec{k}} - \left| v_{\vec{k}} \right|^2 \gamma_{\vec{k}}^+ \gamma_{-\vec{k}} + \left| v_{\vec{k}} \right|^2 \gamma_{\vec{k}}^+ \gamma_{-\vec{k}} + u_{\vec{k}}^+ v_{\vec{k}} \gamma_{\vec{k}} \gamma_{-\vec{k}} \gamma_{\vec{k}}^+ \right) \\
& + \Delta_2 \sum_p u_{\vec{k}} v_{\vec{k}}^+ \gamma_{\vec{k}}^+ - \left| v_{\vec{k}} \right|^2 \gamma_{\vec{k}} \gamma_{-\vec{k}} + u_{\vec{k}}^2 \gamma_{\vec{k}}^+ \gamma_{-\vec{k}} + u_{\vec{k}}^+ v_{\vec{k}} \gamma_{\vec{k}} \gamma_{-\vec{k}} \gamma_{\vec{k}}^+ + \Delta_2 \sum_p -v_{\vec{k}}^+ \gamma_{\vec{k}} + u_{\vec{k}} \gamma_{\vec{k}}^+ \\
& + \left(-v_{\vec{k}}^+ u_{\vec{k}}^+ \gamma_{\vec{k}}^+ \gamma_{-\vec{k}} + \left| u_{\vec{k}} \right|^2 \gamma_{\vec{k}} \gamma_{-\vec{k}} - \left| v_{\vec{k}} \right|^2 \gamma_{\vec{k}} \gamma_{-\vec{k}} + u_{\vec{k}}^+ v_{\vec{k}} \gamma_{\vec{k}} \gamma_{-\vec{k}} \gamma_{\vec{k}}^+ + v_{\vec{k}}^+ \gamma_{\vec{k}} + u_{\vec{k}} \gamma_{\vec{k}}^+ \right) \\
& + u_{\vec{k}} v_{\vec{k}}^+ \gamma_{\vec{k}}^+ \gamma_{-\vec{k}} - \left| v_{\vec{k}} \right|^2 \gamma_{\vec{k}} \gamma_{-\vec{k}} + u_{\vec{k}}^2 \gamma_{\vec{k}}^+ \gamma_{-\vec{k}} + u_{\vec{k}}^+ v_{\vec{k}} \gamma_{\vec{k}} \gamma_{-\vec{k}}
\end{aligned} \tag{4.54}$$

The same operation is done to equation (4.54) by vanishing coefficient to give diagonalised

equation (4.55)

$$\begin{aligned}
H_{pd} = & \Delta_1^+ \sum_d \left(-v_{\vec{k}}^+ u_{\vec{k}}^+ \gamma_{\vec{k}}^+ \gamma_{-\vec{k}} + \gamma_{\vec{k}} \gamma_{-\vec{k}} - \gamma_{\vec{k}}^+ \gamma_{-\vec{k}} + \gamma_{\vec{k}}^+ \gamma_{-\vec{k}} + u_{\vec{k}}^+ v_{\vec{k}} \gamma_{\vec{k}} \gamma_{-\vec{k}} \gamma_{\vec{k}}^+ \right) \\
& + \Delta_2 \sum_p u_{\vec{k}} v_{\vec{k}}^+ \gamma_{\vec{k}}^+ - \gamma_{\vec{k}} \gamma_{-\vec{k}} + \gamma_{\vec{k}}^+ \gamma_{-\vec{k}} + u_{\vec{k}}^+ v_{\vec{k}} \gamma_{\vec{k}} \gamma_{-\vec{k}} \gamma_{\vec{k}}^+ + \Delta_2 \sum_p -v_{\vec{k}}^+ \gamma_{\vec{k}} + u_{\vec{k}} \gamma_{\vec{k}}^+ \\
& + \left(-v_{\vec{k}}^+ u_{\vec{k}}^+ \gamma_{\vec{k}}^+ \gamma_{-\vec{k}} + \gamma_{\vec{k}} \gamma_{-\vec{k}} - \gamma_{\vec{k}} \gamma_{-\vec{k}} + u_{\vec{k}}^+ v_{\vec{k}} \gamma_{\vec{k}} \gamma_{-\vec{k}} \gamma_{\vec{k}}^+ + v_{\vec{k}}^+ \gamma_{\vec{k}} + u_{\vec{k}} \gamma_{\vec{k}}^+ \right) + \\
& u_{\vec{k}} v_{\vec{k}}^+ \gamma_{\vec{k}}^+ \gamma_{-\vec{k}} - \gamma_{\vec{k}} \gamma_{-\vec{k}} + \gamma_{\vec{k}}^+ \gamma_{-\vec{k}} + u_{\vec{k}}^+ v_{\vec{k}} \gamma_{\vec{k}} \gamma_{-\vec{k}}
\end{aligned} \tag{4.55}$$

on collecting like terms, in equation (4.55), it becomes equation (4.56) below.

$$\begin{aligned}
H_{pd} = & \Delta_1^+ \sum_d \left(-v_{\vec{k}}^+ u_{\vec{k}}^+ \gamma_{\vec{k}}^+ \gamma_{-\vec{k}}^+ + \gamma_{\vec{k}}^+ \gamma_{-\vec{k}}^+ + u_{\vec{k}}^+ v_{\vec{k}}^+ \gamma_{\vec{k}}^+ \gamma_{-\vec{k}}^+ \gamma_{\vec{k}}^+ \right) \\
& + \Delta_2 \sum_p u_{\vec{k}}^+ v_{\vec{k}}^+ \gamma_{\vec{k}}^+ \gamma_{-\vec{k}}^+ - \gamma_{\vec{k}}^+ \gamma_{-\vec{k}}^+ + \gamma_{\vec{k}}^+ \gamma_{\vec{k}}^+ + u_{\vec{k}}^+ v_{\vec{k}}^+ \gamma_{\vec{k}}^+ \gamma_{-\vec{k}}^+ + \Delta_2^+ \sum_p -v_{\vec{k}}^+ \gamma_{\vec{k}}^+ + u_{\vec{k}}^+ \gamma_{-\vec{k}}^+ \quad (4.56) \\
& + \left(-v_{\vec{k}}^+ u_{\vec{k}}^+ \gamma_{\vec{k}}^+ \gamma_{-\vec{k}}^+ + u_{\vec{k}}^+ v_{\vec{k}}^+ \gamma_{\vec{k}}^+ \gamma_{-\vec{k}}^+ \gamma_{\vec{k}}^+ + v_{\vec{k}}^+ \gamma_{\vec{k}}^+ + u_{\vec{k}}^+ \gamma_{-\vec{k}}^+ \right) \\
& + u_{\vec{k}}^+ v_{\vec{k}}^+ \gamma_{\vec{k}}^+ \gamma_{-\vec{k}}^+ - \gamma_{\vec{k}}^+ \gamma_{-\vec{k}}^+ + \gamma_{\vec{k}}^+ \gamma_{-\vec{k}}^+ + u_{\vec{k}}^+ v_{\vec{k}}^+ \gamma_{\vec{k}}^+ \gamma_{-\vec{k}}^+
\end{aligned}$$

Putting all terms together in equations (4.50),(4.51) and (4.52) and when the coefficients of

$\gamma_{\vec{k}}^+ \gamma_{-\vec{k}}^+$ and $\gamma_{\vec{k}}^+ \gamma_{\vec{k}}^+$ vanish with the terms, the model Hamiltonian for magnesium diBoride

for phonon-mediated attraction and coulomb repulsion becomes equation (4.57)

$$\begin{aligned}
H_M = & \varepsilon_p \gamma_{\vec{k}}^+ \gamma_{-\vec{k}}^+ \gamma_{\vec{k}}^+ \gamma_{-\vec{k}}^+ - \gamma_{\vec{k}}^+ \gamma_{-\vec{k}}^+ + \varepsilon_d \gamma_{\vec{k}}^+ \gamma_{-\vec{k}}^+ \gamma_{\vec{k}}^+ \gamma_{-\vec{k}}^+ + v_{pd} \gamma_{\vec{k}}^+ \gamma_{-\vec{k}}^+ \gamma_{\vec{k}}^+ \gamma_{-\vec{k}}^+ \gamma_{\vec{k}}^+ \gamma_{-\vec{k}}^+ \\
& + \gamma_{\vec{k}}^+ \gamma_{-\vec{k}}^+ + \gamma_{\vec{k}}^+ \gamma_{-\vec{k}}^+ + \Delta_{pd}^+ u_{\vec{k}}^+ \gamma_{\vec{k}}^+ \gamma_{-\vec{k}}^+ - v_{\vec{k}}^+ \gamma_{\vec{k}}^+ \gamma_{-\vec{k}}^+ \gamma_{\vec{k}}^+ \gamma_{-\vec{k}}^+ \gamma_{\vec{k}}^+ \gamma_{-\vec{k}}^+ \quad (4.57)
\end{aligned}$$

The operators obey the bosonic commutation relationships as per equation (4.59) below

$$\begin{aligned}
\gamma_{\vec{k}}^+ \gamma_{-\vec{k}}^+ &= 0 \\
\gamma_{\vec{k}} \gamma_{-\vec{k}} &= 0 \quad (4.58)
\end{aligned}$$

$$\left[\gamma_{\vec{k}}^+, \gamma_{\vec{k}} \right] = \delta_{\vec{k}} \quad (4.59)$$

Hence equation (4.57) reduces to equation (4.60)

$$H_M = \varepsilon_p \gamma_{\vec{k}}^+ \gamma_{-\vec{k}}^+ \gamma_{\vec{k}}^+ \gamma_{-\vec{k}}^+ + \varepsilon_d \gamma_{\vec{k}}^+ \gamma_{-\vec{k}}^+ \gamma_{\vec{k}}^+ \gamma_{-\vec{k}}^+ + \gamma_{\vec{k}}^+ \gamma_{-\vec{k}}^+ \gamma_{\vec{k}}^+ \gamma_{-\vec{k}}^+ \gamma_{\vec{k}}^+ \gamma_{-\vec{k}}^+ + \Delta_{pd}^+ u_{\vec{k}}^+ \gamma_{\vec{k}}^+ \gamma_{-\vec{k}}^+ \gamma_{\vec{k}}^+ - v_{\vec{k}}^+ \gamma_{\vec{k}}^+ \gamma_{-\vec{k}}^+ \gamma_{\vec{k}}^+ \gamma_{-\vec{k}}^+ \gamma_{\vec{k}}^+ \gamma_{-\vec{k}}^+ \quad (4.60)$$

Then model Hamiltonian in (4.60) is the diagonalized equation by Bogoliubov-Valatin transformation equations. According to (Rapando, Khanna, & Mong'are, 2016), when we considered the particle spin up as k and spin down as $-k$, then scattered spin states will be represented by k and $-k$ for spin up and spin down respectively. By neglecting higher order terms, number operators and off diagonal terms, the diagonalised terms of Hamiltonian becomes equation (4.60)

4.6 Interaction energy

We now calculate the average energy that is required during the interaction using the normalized wave function $|\Psi\rangle$

$$E_n = \langle \Psi | H_M | \Psi \rangle$$

$$\begin{aligned} \langle \Psi | H_M | \Psi \rangle = & \langle 0 | \varepsilon_p \gamma_{\vec{k}}^+ \gamma_{\vec{-k}}^+ \gamma_{\vec{k}} \gamma_{\vec{-k}} + \varepsilon_p \gamma_{\vec{k}}^+ \gamma_{\vec{-k}} \gamma_{\vec{k}}^+ \gamma_{\vec{-k}} + \gamma_{\vec{k}} \gamma_{\vec{-k}} \gamma_{\vec{k}}^+ \gamma_{\vec{-k}}^+ \gamma_{\vec{k}} \gamma_{\vec{-k}}^+ \\ & + \Delta_{pd}^+ u_{\vec{k}}^+ \gamma_{\vec{k}} \gamma_{\vec{-k}} \gamma_{\vec{k}}^+ - v_{\vec{k}} \gamma_{\vec{k}}^+ \gamma_{\vec{-k}}^+ \gamma_{\vec{k}} \gamma_{\vec{-k}} \gamma_{\vec{k}} \gamma_{\vec{-k}} | 0 \rangle \end{aligned} \quad (4.61)$$

Where the vacuum state is represented by $|0\rangle$ has three distinct spaces i.e $|0\rangle = |0_{-k}, 0_k, 0_{k^1}\rangle$

By doing expansion on terms in the equation and performing the bra-ket operator on each term in the bra-ket, followed by factorization, we set equation (4.61) for normalization case by rewriting it as

$$E_g = \langle 0 | u_k \gamma_{\vec{k}}^+ \left(\begin{array}{l} \varepsilon_p \gamma_{\vec{k}}^+ \gamma_{\vec{-k}}^+ \gamma_{\vec{k}} \gamma_{\vec{-k}} \\ + \varepsilon_d \gamma_{\vec{k}}^+ \gamma_{\vec{-k}} \gamma_{\vec{k}}^+ \gamma_{\vec{-k}} \\ + \gamma_{\vec{k}} \gamma_{\vec{-k}} \gamma_{\vec{k}}^+ \gamma_{\vec{-k}}^+ \gamma_{\vec{k}} \gamma_{\vec{-k}}^+ \\ + \Delta_{pd}^+ u_{\vec{k}}^+ \gamma_{\vec{k}} \gamma_{\vec{-k}} \gamma_{\vec{k}}^+ \\ - v \gamma_{\vec{k}}^+ \gamma_{\vec{-k}}^+ \gamma_{\vec{k}} \gamma_{\vec{-k}} \gamma_{\vec{k}} \gamma_{\vec{-k}} \end{array} \right) v_k \gamma_{\vec{k}} | 0 \rangle \quad (4.62)$$

Equation (4.62) can be expanded and simplified as below

$$\begin{aligned}
E_g = & \langle 0 | u_{\vec{k}} \gamma_{\vec{k}}^+ \varepsilon_p \gamma_{\vec{k}}^+ \gamma_{\vec{k}}^+ \gamma_{\vec{k}}^+ \gamma_{\vec{k}}^+ \gamma_{\vec{k}}^+ v_{\vec{k}} \gamma_{\vec{k}} | 0 \rangle \\
& + \langle 0 | u_{\vec{k}} \gamma_{\vec{k}}^+ \varepsilon_p \gamma_{\vec{k}}^+ \gamma_{\vec{k}}^+ \gamma_{\vec{k}}^+ \gamma_{\vec{k}}^+ v_{\vec{k}} \gamma_{\vec{k}} | 0 \rangle \\
& + \langle 0 | u_{\vec{k}} \gamma_{\vec{k}}^+ \gamma_{\vec{k}}^+ \gamma_{\vec{k}}^+ \gamma_{\vec{k}}^+ \gamma_{\vec{k}}^+ \gamma_{\vec{k}}^+ \gamma_{\vec{k}}^+ v_{\vec{k}} \gamma_{\vec{k}} | 0 \rangle \\
& + \langle 0 | u_{\vec{k}} \gamma_{\vec{k}}^+ \Delta_{pd}^+ u_{\vec{k}}^+ \gamma_{\vec{k}}^+ \gamma_{\vec{k}}^+ \gamma_{\vec{k}}^+ v_{\vec{k}} \gamma_{\vec{k}} | 0 \rangle \\
& - \langle 0 | u_{\vec{k}} \gamma_{\vec{k}}^+ v_{\vec{k}} \gamma_{\vec{k}}^+ \gamma_{\vec{k}}^+ \gamma_{\vec{k}}^+ \gamma_{\vec{k}}^+ \gamma_{\vec{k}}^+ \gamma_{\vec{k}}^+ v_{\vec{k}} \gamma_{\vec{k}} | 0 \rangle
\end{aligned} \tag{4.63}$$

The vacuum state represented by $|0\rangle$ has three distinct spaces i.e $|0\rangle = |0_{-k}, 0_k, 0_{k^1}\rangle$

Hence we rewrite equation (4.63) as

$$\begin{aligned}
E_g = & \langle 0_k 0_{-k} 0_{k^1} | u_{\vec{k}} \gamma_{\vec{k}}^+ \varepsilon_p \gamma_{\vec{k}}^+ \gamma_{\vec{k}}^+ \gamma_{\vec{k}}^+ \gamma_{\vec{k}}^+ v_{\vec{k}} \gamma_{\vec{k}} | 0_k 0_{-k} 0_{k^1} \rangle \\
& + \langle 0_k 0_{-k} 0_{k^1} | u_{\vec{k}} \gamma_{\vec{k}}^+ \varepsilon_p \gamma_{\vec{k}}^+ \gamma_{\vec{k}}^+ \gamma_{\vec{k}}^+ v_{\vec{k}} \gamma_{\vec{k}} | 0_k 0_{-k} 0_{k^1} \rangle \\
& + \langle 0_k 0_{-k} 0_{k^1} | u_{\vec{k}} \gamma_{\vec{k}}^+ \gamma_{\vec{k}}^+ \gamma_{\vec{k}}^+ \gamma_{\vec{k}}^+ \gamma_{\vec{k}}^+ \gamma_{\vec{k}}^+ v_{\vec{k}} \gamma_{\vec{k}} | 0_k 0_{-k} 0_{k^1} \rangle \\
& + \langle 0_k 0_{-k} 0_{k^1} | u_{\vec{k}} \gamma_{\vec{k}}^+ \Delta_{pd}^+ u_{\vec{k}}^+ \gamma_{\vec{k}}^+ \gamma_{\vec{k}}^+ v_{\vec{k}} \gamma_{\vec{k}} | 0_k 0_{-k} 0_{k^1} \rangle \\
& - \langle 0_k 0_{-k} 0_{k^1} | u_{\vec{k}} \gamma_{\vec{k}}^+ v_{\vec{k}} \gamma_{\vec{k}}^+ \gamma_{\vec{k}}^+ \gamma_{\vec{k}}^+ \gamma_{\vec{k}}^+ \gamma_{\vec{k}}^+ v_{\vec{k}} \gamma_{\vec{k}} | 0_k 0_{-k} 0_{k^1} \rangle
\end{aligned} \tag{4.64}$$

Noting that $\gamma^+ |0\rangle = |1\rangle$, $\gamma |0\rangle = 0$, and $\gamma |1\rangle = |0\rangle$, then equation (4.64) is simplified to

$$\begin{aligned}
E_g = & \langle 0_k 0_{-k} 0_{k^1} | v_{\vec{k}} \gamma_{\vec{k}}^+ \varepsilon_p v_{\vec{k}} \gamma_{\vec{k}} | 0_k 0_{-k} 0_{k^1} \rangle \\
& + \langle 0_k 0_{-k} 0_{k^1} | u_{\vec{k}} \gamma_{\vec{k}}^+ \varepsilon_p u_{\vec{k}} \gamma_{\vec{k}} | 0_k 0_{-k} 0_{k^1} \rangle \\
& + \langle 0_k 0_{-k} 0_{k^1} | \gamma_{\vec{k}}^+ \gamma_{\vec{k}} | 0_k 0_{-k} 0_{k^1} \rangle \\
& + \langle 0_k 0_{-k} 0_{k^1} | u_{\vec{k}} \gamma_{\vec{k}}^+ \Delta_{pd}^+ u_{\vec{k}}^+ v_{\vec{k}} \gamma_{\vec{k}} | 0_k 0_{-k} 0_{k^1} \rangle \\
& - \langle 0_k 0_{-k} 0_{k^1} | u_{\vec{k}} \gamma_{\vec{k}}^+ v_{\vec{k}} v_{\vec{k}} \gamma_{\vec{k}} | 0_k 0_{-k} 0_{k^1} \rangle
\end{aligned} \tag{4.65}$$

$$\begin{aligned}
E_g &= \langle \mathbf{0}_k \mathbf{0}_{-k} \mathbf{0}_{k^1} | \varepsilon_p v_k^2 \gamma_k^+ \gamma_k^- | \mathbf{0}_k \mathbf{0}_{-k} \mathbf{0}_{k^1} \rangle \\
&+ \langle \mathbf{0}_k \mathbf{0}_{-k} \mathbf{0}_{k^1} | \varepsilon_d u_k^2 \gamma_k^+ \gamma_k^- | \mathbf{0}_k \mathbf{0}_{-k} \mathbf{0}_{k^1} \rangle \\
&+ \langle \mathbf{0}_k \mathbf{0}_{-k} \mathbf{0}_{k^1} | \gamma_k^+ \gamma_k^- | \mathbf{0}_k \mathbf{0}_{-k} \mathbf{0}_{k^1} \rangle \\
&+ \langle \mathbf{0}_k \mathbf{0}_{-k} \mathbf{0}_{k^1} | \Delta_{pd}^+ u_k^2 v_k^- \gamma_k^+ \gamma_k^- | \mathbf{0}_k \mathbf{0}_{-k} \mathbf{0}_{k^1} \rangle \\
&- \langle \mathbf{0}_k \mathbf{0}_{-k} \mathbf{0}_{k^1} | v_k^2 u_k^- \gamma_k^+ \gamma_k^- | \mathbf{0}_k \mathbf{0}_{-k} \mathbf{0}_{k^1} \rangle
\end{aligned} \tag{4.66}$$

$$\begin{aligned}
E_g &= \langle \mathbf{0}_k \mathbf{0}_{-k} \mathbf{0}_{k^1} | \varepsilon_p v_k^2 | \mathbf{0}_k \mathbf{0}_{-k} \mathbf{0}_{k^1} \rangle \\
&+ \langle \mathbf{0}_k \mathbf{0}_{-k} \mathbf{0}_{k^1} | \varepsilon_d u_k^2 | \mathbf{0}_k \mathbf{0}_{-k} \mathbf{0}_{k^1} \rangle \\
&+ \langle \mathbf{0}_k \mathbf{0}_{-k} \mathbf{0}_{k^1} | 0 | \mathbf{0}_k \mathbf{0}_{-k} \mathbf{0}_{k^1} \rangle \\
&+ \langle \mathbf{0}_k \mathbf{0}_{-k} \mathbf{0}_{k^1} | \Delta_{pd}^+ u_k^2 v_k^- | \mathbf{0}_k \mathbf{0}_{-k} \mathbf{0}_{k^1} \rangle \\
&- \langle \mathbf{0}_k \mathbf{0}_{-k} \mathbf{0}_{k^1} | v_k^2 u_k^- | \mathbf{0}_k \mathbf{0}_{-k} \mathbf{0}_{k^1} \rangle
\end{aligned} \tag{4.67}$$

Noting that $\langle \mathbf{0}_k \mathbf{0}_{-k} \mathbf{0}_{k^1} | \mathbf{0}_k \mathbf{0}_{-k} \mathbf{0}_{k^1} \rangle = 1$

Then equation (4.67) is simplified to

$$\begin{aligned}
E_g &= \varepsilon_p v_k^2 \langle \mathbf{0}_k \mathbf{0}_{-k} \mathbf{0}_{k^1} | \mathbf{0}_k \mathbf{0}_{-k} \mathbf{0}_{k^1} \rangle \\
&+ \varepsilon_d u_k^2 \langle \mathbf{0}_k \mathbf{0}_{-k} \mathbf{0}_{k^1} | \mathbf{0}_k \mathbf{0}_{-k} \mathbf{0}_{k^1} \rangle \\
&+ 0 \langle \mathbf{0}_k \mathbf{0}_{-k} \mathbf{0}_{k^1} | \mathbf{0}_k \mathbf{0}_{-k} \mathbf{0}_{k^1} \rangle \\
&+ \Delta_{pd}^+ u_k^2 v_k^- \langle \mathbf{0}_k \mathbf{0}_{-k} \mathbf{0}_{k^1} | \mathbf{0}_k \mathbf{0}_{-k} \mathbf{0}_{k^1} \rangle \\
&- v_k^2 u_k^- \langle \mathbf{0}_k \mathbf{0}_{-k} \mathbf{0}_{k^1} | \mathbf{0}_k \mathbf{0}_{-k} \mathbf{0}_{k^1} \rangle
\end{aligned} \tag{4.68}$$

$$E_g = \varepsilon_p v_k^2 + \varepsilon_d u_k^2 + 0 + \Delta_{pd}^+ u_k^2 v_k^- - v_k^2 u_k^- \tag{4.69}$$

$$E_g = \varepsilon_p v_k^2 + \varepsilon_d u_k^2 + \Delta_{pd}^+ u_k^2 v_k^- - v_k^2 u_k^- \tag{4.70}$$

Assuming that the kinetic energy at vacuum state for p-band, d-band and interaction term pd between bands are equal, then;

$$\varepsilon_p = \varepsilon_d = \varepsilon_{pd} \quad (4.71)$$

then

$$E_g = \varepsilon_{pd} \left(v_{\vec{k}}^2 + u_{\vec{k}}^2 \right) + \Delta_{\vec{k}}^+ u_{\vec{k}}^2 v_{\vec{k}} - v_{\vec{k}}^2 u_{\vec{k}} \quad (4.72)$$

therefore

$$E_g = \varepsilon_{pd} + \Delta_{\vec{k}}^+ u_{\vec{k}}^2 v_{\vec{k}} - v_{\vec{k}}^2 u_{\vec{k}} \quad (4.73)$$

Equation (4.73) is the energy of state for two band model, the case of magnesium diboride where E_g is the total ground state energy. It differs from energy of one band model due the additional $\varepsilon_{pd} + \Delta_{\vec{k}}^+$ terms of energy showing the lowest energy achieved in the p and d bands at vacuum state, indicating formation of the bands at lowest energy in the system.

ε_{pd} energy in p and d bands

$\Delta_{\vec{k}}^+ u_{\vec{k}}^2 v_{\vec{k}}$ interactive potential between the p and d bands

$v_{\vec{k}}^2 u_{\vec{k}}$ enhanced coulomb energy between bosons as they interact

The two band model possess lower energy at vacuum state compared to one band model superconductor, hence bosons can be formed at lowest energy of magnesium diboride.

In relating the above energy with temperature, we multiply equation (4.73) with thermal activation factor equation (4.74) that does not change energy value but only relates it with temperature, to get equation (4.75) where $100K_B T$ is due to two band nature of MgB_2 .

$$e^{-E_g/100K_B T} \quad (4.74)$$

$$E_n = E_g e^{-E_g/100K_B T} \quad (4.75)$$

Therefore the energy of the system of magnesium diBoride is given as in equation (4.76)

$$E_n = (\varepsilon_{pd} + \Delta_k^+ u_k^2 v_k - v_k^2 u_k) e^{-(\varepsilon_{pd} + \Delta_k^+ u_k^2 v_k - v_k^2 u_k)/100K_B T} \quad (4.76)$$

1.7 Specific heat capacity.

The formulawas derived for finding specific heat capacity for magnesium diBoride system for interaction of electrons in the two bands from the generalized standard equation (4.77).

$$C_V = \frac{dE_n}{dT} \quad (4.77)$$

β was introduced

$$\beta = (\varepsilon_{pd} + \Delta_k^+ u_k^2 v_k - v_k^2 u_k)/100K_B \quad (4.78)$$

Equation (4.78) is substituted into equation (4.75) to get equation (4.79).

$$E_n = (\varepsilon_{pd} + \Delta_k^+ u_k^2 v_k - v_k^2 u_k) e^{-\beta/T} \quad (4.79)$$

The let $t = \frac{\beta}{T}$

$$\text{Therefore } E_n = (\varepsilon_{pd} + \Delta_k^+ u_k^2 v_k - v_k^2 u_k) e^{-t} \quad (4.80)$$

$$E_n = E_g e^t$$

$$\frac{dt}{dT} = -\frac{\beta}{T^2} \quad (4.81)$$

$$\text{Hence } dt = \frac{-\beta}{T^2} dT$$

Then

$$dT = \frac{-T^2}{\beta} dt \quad (4.82)$$

Substituting equation (4.79) into equation (4.77), we get equation (4.83)

$$C_V = \frac{d(\varepsilon_{pd} + \Delta_k^+ u_k^2 v_k - v_k^2 u_k) e^t}{100 dT}$$

$$\text{but } dt = \frac{-\beta}{T^2} dT$$

$$C_V = \frac{d}{\frac{-100T^2}{\beta} dt} (\varepsilon_{pd} + \Delta_k^+ u_k^2 v_k - v_k^2 u_k) e^t$$

$$C_V = \frac{\beta(\varepsilon_{pd} + \Delta_k^+ u_k^2 v_k - v_k^2 u_k)}{-100K_B T^2} e^t \quad (4.83)$$

We now substituted the values of t and β into equation (4.77)

$$C_V = \frac{(\varepsilon_{pd} + \Delta_k^+ u_k^2 v_k - v_k^2 u_k)^2}{-100K_B T^2} e^{-(\varepsilon_{pd} + \Delta_k^+ u_k^2 v_k - v_k^2 u_k)/100K_B T} \quad (4.84)$$

The equation (4.84) is the specific heat formula.

4.8 Somerfield coefficient and entropy

We now solve for Somerfield coefficient γ which is derived from the specific heat formula

$$\gamma = \frac{C_V}{T}$$

$$\gamma = \frac{(\varepsilon_{pd} + \Delta_k^+ u_k^2 v_k - v_k^2 u_k)^2}{-100K_B T^2} e^{-(\varepsilon_{pd} + \Delta_k^+ u_k^2 v_k - v_k^2 u_k)/100K_B T} / T$$

$$\gamma = \frac{(\varepsilon_{pd} + \Delta_k^+ u_k^2 v_k - v_k^2 u_k)^2}{-100K_B T} e^{-(\varepsilon_{pd} + \Delta_k^+ u_k^2 v_k - v_k^2 u_k)/100K_B T} \quad (4.85)$$

Entropy is derived from equation (4.84), given as

$$S = \int C_V \frac{dT}{T} \quad (4.86)$$

$$S = \int \frac{(\varepsilon_{pd} + \Delta_k^+ u_k^2 v_k - v_k^2 u_k)^2}{-100K_B T} e^{-(\varepsilon_{pd} + \Delta_k^+ u_k^2 v_k - v_k^2 u_k)/100K_B T} \frac{dT}{T}$$

$$S = \int \frac{(\varepsilon_{pd} + \Delta_k^+ u_k^2 v_k - v_k^2 u_k)^2}{100K_B T} e^{-(\varepsilon_{pd} + \Delta_k^+ u_k^2 v_k - v_k^2 u_k)/100K_B T} dT \quad (4.87)$$

$$\text{We let } t = \frac{(\varepsilon_{pd} + \Delta_k^+ u_k^2 v_k - v_k^2 u_k)}{100K_B T} \quad (4.88)$$

$$\frac{dt}{dT} = \frac{\varepsilon_{pd} + \Delta_k^+ u_k^2 v_k - v_k^2 u_k}{100K_B T} \quad (4.89)$$

Which means when you make dT the subject of the formulae

$$dT = \frac{100K_B T^2}{\varepsilon_{pd} + \Delta_k^+ u_k^2 v_k - v_k^2 u_k} dt \quad (4.90)$$

Therefore entropy equation is got by substituting equation (4.90) into equation (4.87) to get equation (4.91)

$$S = \int \frac{(\varepsilon_{pd} + \Delta_k^+ u_k^2 v_k - v_k^2 u_k)^2}{100K_B T^3} e^{-(\varepsilon_{pd} + \Delta_k^+ u_k^2 v_k - v_k^2 u_k)/100K_B T} \cdot \frac{100K_B T^2}{(\varepsilon_{pd} + \Delta_k^+ u_k^2 v_k - v_k^2 u_k)} \quad (4.91)$$

When simplified

$$S = \int \frac{(\varepsilon_{pd} + \Delta_k^+ u_k^2 v_k - v_k^2 u_k)^2}{100K_B T^3} e^{-(\varepsilon_{pd} + \Delta_k^+ u_k^2 v_k - v_k^2 u_k)/100K_B T} \cdot \frac{100K_B T^2}{(\varepsilon_{pd} + \Delta_k^+ u_k^2 v_k - v_k^2 u_k)} dt \quad (4.92)$$

$$S = \int \frac{(\varepsilon_{pd} + \Delta_k^+ u_k^2 v_k - v_k^2 u_k)}{100K_B T} e^{-(\varepsilon_{pd} + \Delta_k^+ u_k^2 v_k - v_k^2 u_k)/100K_B T} dt \quad (4.93)$$

From relation in equation (4.88)

$$\text{We note that } \frac{(\varepsilon_{pd} + \Delta_k^+ u_k^2 v_k - v_k^2 u_k)}{T} = 100K_B t \quad (4.94)$$

$$S = \int (-k_B t) e^t dt = K_B \int t e^t dt \quad (4.95)$$

Integration by parts, where we let

$U=t$ and $e^t dt = dv$, we get

$$\begin{aligned} \int u dv &= uv - \int v du \\ \int t e^t dt &= t e^t - \int e^t dt \\ &= t e^t - e^t + C \end{aligned} \quad (4.96)$$

$$\begin{aligned} S &= -100K_B \int t e^t dt \\ &= -100K_B (t e^t - e^t + C) \\ &= -100K_B e^t (1-t) + C \end{aligned}$$

$$S = -100K_B e^{-(\varepsilon_{pd} + \Delta_k^+ u_k^2 v_k - v_k^2 u_k) / 100K_B T} \left(1 + \frac{\varepsilon_{pd} + \Delta_k^+ u_k^2 v_k - v_k^2 u_k}{100K_B T} \right)$$

$$S = 100K_B \left(1 + \frac{\varepsilon_{pd} + \Delta_k^+ u_k^2 v_k - v_k^2 u_k}{100K_B T} \right) e^{-(\varepsilon_{pd} + \Delta_k^+ u_k^2 v_k - v_k^2 u_k) / 100k_B T} \quad (4.97)$$

Equation (4.97) represents entropy in two band model.

4.9. Transition temperature T_c

To calculate the transition temperature, equation (4.97) is reduced to equation (4.98) as bellow

by first letting the value of $T=T_c$, and use of derived equation for specific heat capacity (4.84)

and energy of the system (4.76) together with Boltzeman's constant K_B

$$\left(\frac{\partial \left(\frac{(\varepsilon_{pd} + \Delta_k^+ u_k^2 v_k - v_k^2 u_k)^2}{100 K_B T^2} e^{-\frac{(\varepsilon_{pd} + \Delta_k^+ u_k^2 v_k - v_k^2 u_k)}{100 K_B T}} \right)}{\partial T} \right)_{T=T_C} = - \frac{2(\varepsilon_{pd} + \Delta_k^+ u_k^2 v_k - v_k^2 u_k)^2}{100 K_B T_C^3} e^{\frac{(\varepsilon_{pd} + \Delta_k^+ u_k^2 v_k - v_k^2 u_k)}{100 K_B T_C}}$$

$$+ \frac{(\varepsilon_{pd} + \Delta_k^+ u_k^2 v_k - v_k^2 u_k)^3}{100 K_B^2 T_C^4} e^{\frac{(\varepsilon_{pd} + \Delta_k^+ u_k^2 v_k - v_k^2 u_k)}{100 K_B T_C}} = 0 \quad (4.98)$$

Which means that

$$\frac{2(\varepsilon_{pd} + \Delta_k^+ u_k^2 v_k - v_k^2 u_k)^2}{100 K_B T_C^3} - e^{\frac{(\varepsilon_{pd} + \Delta_k^+ u_k^2 v_k - v_k^2 u_k)}{100 K_B T_C}} = \frac{(\varepsilon_{pd} + \Delta_k^+ u_k^2 v_k - v_k^2 u_k)^3}{100 K_B^2 T_C^4} e^{\frac{-(\varepsilon_{pd} + \Delta_k^+ u_k^2 v_k - v_k^2 u_k)}{100 K_B T_C}}$$

On further simplification

$$T_C = \frac{(\varepsilon_{pd} + \Delta_k^+ u_k^2 v_k - v_k^2 u_k)}{100 K_B} \quad (4.99)$$

Equation (4.99) represents the transition temperature T_C

This finding is non-ceramic with great prospects of practical solutions being cooled by liquid nitrogen as opposed to conventional superconducting materials having been cooled by more expensive liquid helium. We can note that ceramic superconductors are not easy to process due to their brittleness. Brittleness property has limited wide applications like in hospitals for superconducting magnets used in magnetic resonance imaging (MRI) apparatus that helps in generation of large magnetic field necessary for exciting and then atomic image nuclei in body tissues. This will lead to wires with high efficient superconducting magnets and low-loss electric power transmission lines with advanced devices like Josephson junctions in SQUIDS (superconducting quantum interference devices)

According to (Kibe et al 2005) the superconducting electron system is considered as being in one condensed phase and the scattered pairs of electrons are in one s-state singlet pairing and s-state triplet pairing, where electrons are paired so as to minimize the ground state energy.

Where the pairing superconductors' states are considered to be both singlet and triplet, the state is expressed in terms of new operators. This is then diagonalized to obtain the elements of the Hamiltonian that corresponds to stationary states where the system is in equilibrium making use of Bogoliubov-Volatin transformations to transform the equation. It is understood that certain types of interactions can lead to massive quassi-particles such that the resulting effective masses of electrons may reach values between 100 and 1000 times the mass of free electrons. The effective Hamiltonian is diagonalized using the Bogoliubov-Volatin transformations and thermodynamic properties of such heavy fermion system are calculated. The total energy is found to increase with increase in temperature while entropy also changes continuously through the transition temperature T_C , where the entropy of the system decreases with temperature as is conventionally the case. The Hamiltonian H of the system will contain the kinetic energy term, the interaction term due singlet and triplet pairing as according to (Rapando, Khanna, & Mong'are, 2016). To get the quasiparticles of the heavy-Fermion superconducting state, the Hamiltonian H , will be diagonalized using the Bogoliubov-Volatin canonical transformations (Bogoliubov, 1947). The energy of the system, the specific heat C , the entropy S and the transition temperature T_C were calculated. This result is compared to available information in the literature.

Bogoliubov-Volatin canonical transformations were useful in finding solutions of BCS theory in homogeneous system. It's an isomorphism of either the canonical commutation relations algebra or canonical ant-commutation relation algebra, this induces auto equivalence on the respective representations. The model used it to diagonalize Hamiltonians which yield stationary solutions corresponding to Schrodinger equation that corresponds to transformation of the state function. Operator eigen values were calculated with the diagonalized Hamiltonians with corresponding transformations of the state function.

4.11. Density of State and Temperature.

The general equation for density of state for the system is given as below according to (Martins, 2006)

$$D_n(E_n) = \frac{d_n(E_n)}{dE} \quad (4.101)$$

Where $D_n(E)$ is the volume occupied by states and

$$T_F = \frac{E_F}{K_B} \quad (4.102)$$

Where; E_F is the Fermi energy

K_B is Boltzman constant

T_F is the Fermi temperature

$$D_1(E_n) = \frac{1}{C_K} \text{ for one-dimension density of states,}$$

$$D_2(E_n) = \frac{2\pi}{C_k^2(E_n - E_0)} \text{ for two-dimensional density of states,}$$

$$D_3(E_n) = \frac{4\pi}{C_K^3(E_n - E_0)^2} \text{ for three-dimensional density of states.}$$

In condensed matter physics, the density of states of a system describes the number of states that are available to be occupied by the system at each energy level. It is represented as a distribution by a probability density function and is generally an average over the space and time domains of the various states occupied by the system.(Tinkham, 2004)

The distribution function for the E_F ,

$$U = \int E f(E_n) g(E_n) dE_n. \quad (4.103)$$

Where $u = E_F$ when $T=0$ and μ is the internal energy.

Therefore

Substituting equation of $f(E_n)$ into equation of μ , we get

$$U = \int E_n \left(\frac{1}{\exp\left(\frac{E_n - \mu}{K_B T}\right) - 1} \right) g(E_n) dE_n \quad (4.104)$$

$$U = D_n \int E_n \left(\frac{1}{e^{\left(\frac{E_n - \mu}{K_B T}\right)} - 1} \right) g(E_n) dE_n \quad (4.105)$$

$$\frac{U}{D_n} = \int E_n \left(\frac{1}{\exp\left(\frac{E_n - \mu}{K_B T}\right)} \right) dE_n \quad (4.106)$$

$$\frac{1}{D_n} = \frac{\int E_n \cdot \frac{1}{\exp\left(\frac{E_n - \mu}{K_B T}\right)} dE_n}{U} \quad (4.107)$$

$$D_n = \frac{U}{\int E_n \cdot \frac{1}{\exp\left(\frac{E_n - \mu}{K_B T}\right)} dE_n} \quad (4.108)$$

Equation (4.108) is the expression for variation of density of state D_n and temperature T , for high T_C superconductors in two band models.

CHAPTER FIVE

RESULTS, ANALYSIS AND DISCUSSION

5.1 Numerical Calculations and Results

Various physical properties of MgB₂ can be studied through numerical equations for a given system of results. Numerical evaluation for ground state energy, specific heat, entropy and T_c values for MgB₂ two band superconductor were calculated.

the Considered;

Energy gap range at vacuum state $\Delta_0(0) = 1.8 - 7.5 eV$ table 2.1 (page 26),

Phonon energy range ε_{pd} given as 0.00875eV-0.00937eV from table 2.3, page 36

With calculated values for v_k and u_k from the ground state energy E_g as given in equation (4.73)

By setting two conditions of E_g by setting it to zero, with values of energy gap and phonon energy picked within the ranges given above the following equation are gotten;

$$0.00875eV + 2.4249u_{\vec{k}}^2v_{\vec{k}} - v_{\vec{k}}^2u_{\vec{k}} = 0$$

$$0.00937eV + 2.42u_{\vec{k}}^2v_{\vec{k}} - v_{\vec{k}}^2u_{\vec{k}} = 0$$

Calculation for the values of u_k and v_k was done

$$v_k = 0.92812eV \text{ and } u_k = 0.3723eV$$

That satisfies the condition as given in equation (4.44)

5.2. Ground State Energy

The ground state energy was calculated as follows as given in equation (4.73),

$$E_g = 0.00937eV + 5.616eV(0.3723^2 \times 0.92812) - (0.92812^2 \times 0.3723)$$

$$E_g = 0.00937eV + 5.616eV(0.128644198) - (0.3207017272)$$

$$E_g = 0.4111340888eV$$

Total energy was calculated as given in equation (4.75)

$$E_n = 0.4111340888e^{\frac{0.4111340888}{100 \times 0.00008625 \times 39}}$$

$$E_n = 0.4111340888e^{-0.85271}$$

$$E_n = 0.7670001738eV$$

5.3. Specific Heat Capacity Calculations

Specific heat capacity was calculated as given in equation (4.84)

$$C_V = \frac{E_g^2}{100K_B T^2} e^{-\frac{E_g}{100k_B T}}$$

$$C_V = \frac{0.4111340888^2}{100 \times 0.00008625 \times 39^2} e^{-\frac{0.4111340888}{100 \times 0.00008625 \times 39}}$$

$$C_V = 0.0128848289e^{-1.222492421}$$

$$C_V = 0.0192729906eV / K$$

5.4. Calculations for Entropy

Entropy was calculated from equation (4.97)

$$S = 100 \times 0.00008625 \left(1 + \frac{0.4111340888}{100 \times 0.00008625 \times 39} \right) e^{-\frac{0.4111340888}{100 \times 0.00008625 \times 39}}$$

$$S = 2.2222492421e^{-1.222492421}$$

$$S = 3.3245572813 eV / K$$

5.5. Predicted and calculated transition temperature Tc

As given in equation (4.99), transition temperature was calculated,

$$T_C = \frac{0.4111340888}{100 \times 0.00008625}$$

$$T_C = 47.667720441K$$

5.1.1 Superconducting order parameter

Order parameter for MgB₂ system within two band model, research found the following situations.

The superconducting parameter for p- and d- bands using the equation bellow

$$\frac{V_{pd}(\bar{\Delta}_d)}{\left[1 - V_{pp}(\bar{\Delta}_p)\right]} X \frac{V_{pd}(\bar{\Delta}_p)}{\left[1 - V_{pp}(\bar{\Delta}_d)\right]} = 1 \quad (5.10)$$

$$\text{And } \bar{\Delta} = \bar{\Delta}_p + \bar{\Delta}_d = (V_{pd} + V_{pp}) \left(\bar{\Delta}_p \right) + \left(\bar{\Delta}_d \right) \quad (5.11)$$

Solving the above equation numerically, the study of variation of superconducting order

parameter $\bar{\Delta}_p$ and $\bar{\Delta}_d$ with temperature corresponding Π and σ bands.

$$\bar{\Delta} = \frac{V_{pd} N_d(0) \int_0^1 \frac{dy}{\sqrt{y^2 + 0.5102x^2}} \left[\frac{1}{\exp \frac{-102}{T} \sqrt{y^2 + 0.5102x^2} + 1} - \frac{1}{\exp \frac{102}{T} \sqrt{y^2 + 0.5102x^2} + 1} \right]}{\left[1 - V_{pp} N_p(0) \int_0^1 \frac{dy}{\sqrt{y^2 + 0.4444x^2}} \left[\frac{1}{\exp \frac{-108}{T} \sqrt{y^2 + 0.4444x^2} + 1} - \frac{1}{\exp \frac{108}{T} \sqrt{y^2 + 0.4444x^2} + 1} \right] \right]} X \frac{V_{pd} N_d(0) \int_0^1 \frac{dy}{\sqrt{y^2 + 0.4444x^2}} \left[\frac{1}{\exp \frac{-108}{T} \sqrt{y^2 + 0.4444x^2} + 1} - \frac{1}{\exp \frac{10}{T} \sqrt{y^2 + 0.4444x^2} + 1} \right]}{\left[1 - V_{pp} N_p(0) \int_0^1 \frac{dy}{\sqrt{y^2 + 0.5102x^2}} \left[\frac{1}{\exp \frac{-102}{T} \sqrt{y^2 + 0.5102x^2} + 1} - \frac{1}{\exp \frac{102}{T} \sqrt{y^2 + 0.5102x^2} + 1} \right] \right]} = 1 \quad (5.12)$$

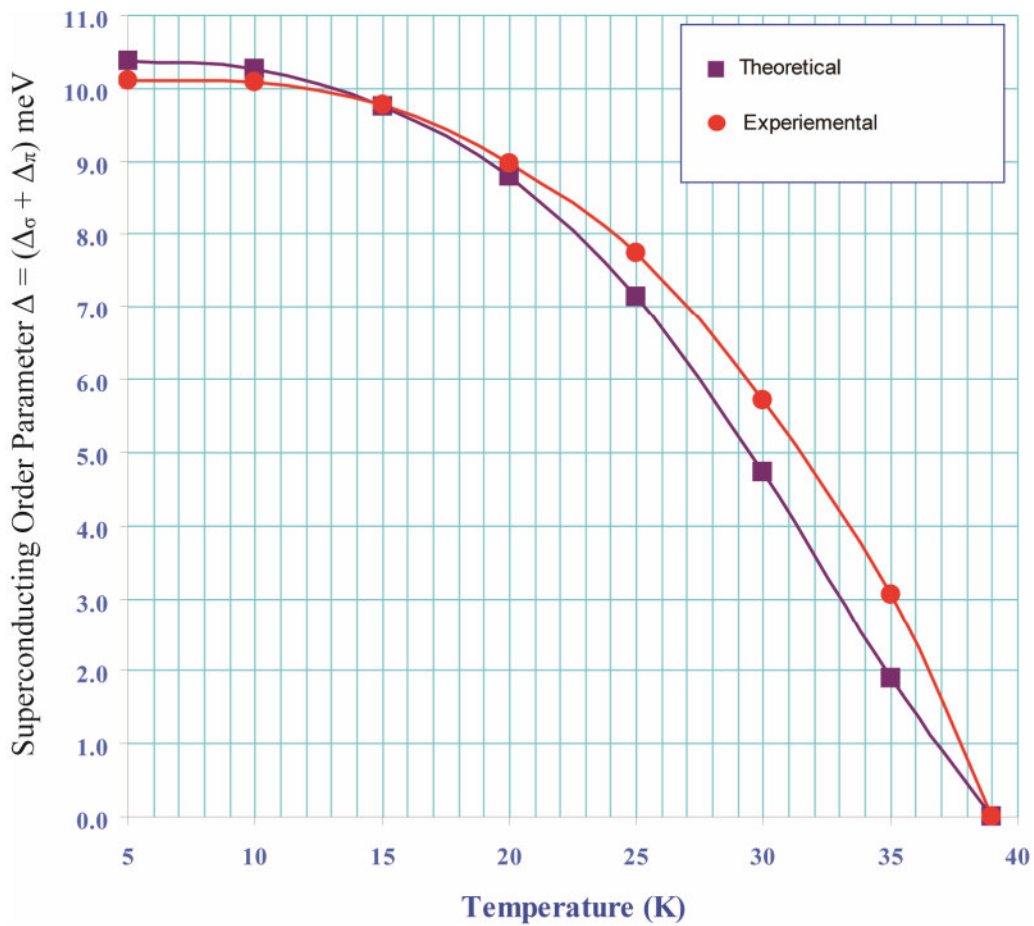
The behavior of superconducting order parameters corresponding with temperature can be seen, the superconducting order parameters for the combined π and σ bands can be studied by taking

simple sum of both parameters. By taking the sum of order parameters $\bar{\Delta} = \bar{\Delta}_{\Pi} + \bar{\Delta}_{\sigma}$, one can

obtain solving the values numerically. A comparison of $\bar{\Delta}$ with BCS type curve is given.

Using equation (5.12), the variation of superconducting order parameter against temperature was studied using Mathcad software and results tabulated and graph drawn as shown.

Figure 5.1 Variation of superconducting order parameter for p and d bands with temperature.



The trend of the graphs is nonlinear in decrease in values of superconducting order parameter in micro electron Volt with increase in temperature in kelvin up to 39k, where the value of order parameter is almost zero but not zero.

Two graphs coincide at 15K and interchange but maintain the trend.

From the graph, order parameter exhibits as wave function for superconductivity at quantum state on microscopic scale.

In the absence of magnetic field $\psi \neq 0$ at $T < T_C$ and $\psi = 0$ at $T > T_C$ and $-\psi = 0$ outside a superconductor.

The order parameter is usually normalized such that $\psi_{(r)}^* \psi_{(r)}$ gives the number density of cooper pairs at point r.

5.1.2 Electronic specific heat (Ces)

The electronic specific heat per atom of a superconductor is determined from the relation

1. For pi bands

$$C_{es}^p = \frac{\partial}{\partial T} \frac{1}{N} \sum_p 2(\epsilon_p - \mu) \langle C_{p\uparrow}^+ C_{p\uparrow} \rangle \quad (5.13)$$

Where ϵ is the energy of pi band and μ is the common chemical potential.

Substituting $\langle C_{p\uparrow}^+ C_{p\uparrow} \rangle$ and changing the summation over p into an integration by using

the relation $\sum_p = N \int_0^{\hbar\omega_p} d\epsilon_p$ we obtained

$$C_{es}^p = \frac{2N(0)}{N} \int_0^{\hbar\omega_p} d\epsilon_p \left\{ \frac{\beta \epsilon_p \alpha_2 \exp(\beta\alpha_2)}{T \{ \exp(\beta\alpha_2) + 1 \}^2} + \frac{\beta(\alpha - \epsilon_1 - \epsilon_p)}{2T \sqrt{\epsilon_p^2 + \Delta_{pp}^2 + \Delta_2^2 + \Delta_{pp}\Delta_2^+ + \Delta_2\Delta_{pp}^+}} \right\} \quad (5.14)$$

Using the above equation after simplification and replacing $\beta = \frac{-1}{K_B T}$, we obtained

$$C_{es}^p = \frac{N(0)}{2NK_B T^2} \int_0^{\hbar\omega_p} d\epsilon_p \epsilon_p^2 \sec h^2 \left(\frac{\sqrt{\epsilon_p^2} + \sqrt{\Delta_p^2}}{2K_B T} \right) \quad (5.15)$$

Changing the phonon energy variables as $\epsilon_p = \hbar\omega_p y$, $d\epsilon_p = \hbar\omega_p dy$ and using parameters in table 2.3 and taking $\mu = 0$, we obtain

$$C_{es}^p = \frac{12.105x10^{-44}}{T^2} \int_0^1 y^2 dy \sec h^2 \left(\frac{36.25\sqrt{2.25y^2 + x^2}}{T} \right) \quad (5.16)$$

For sigma band, we write the expression for specific heat for sigma band

$$C_{es}^d = \frac{9.84x10^{-44}}{T^2} \int_0^1 y^2 \sec h^2 \left(\frac{36.23\sqrt{1.96y^2 + x^2}}{T} \right) \quad (5.17)$$

$$C_{es}^d = \frac{1.2105x10^{-43}}{T^2} \cdot \frac{1}{3} \cdot \sec h^2 \left(\frac{36.25\sqrt{2.25y^2 + x^2}}{T} \right) \quad (5.18)$$

$$C_{es}^d = \frac{1.2105x10^{-43}}{3T^2} \cdot \sec(6.62x10^{-34})^2 \cdot \left(\frac{36.25\sqrt{2.25y^2 + x^2}}{T} \right) \quad (5.19)$$

$$C_{es}^d = \frac{1.2105x10^{-43}}{3T^2} \cdot \sec 4.304x10^{-67} \cdot \left(\frac{36.25\sqrt{2.25y^2 + x^2}}{T} \right) \quad (5.20)$$

$$C_{es}^d = \frac{1.2105x10^{-43}}{3T^2} \cdot \frac{1}{\cos 4.304x10^{-67}} \cdot \left(\frac{36.25\sqrt{2.25y^2 + x^2}}{T} \right) \quad (5.21)$$

$$C_{es}^d = \frac{1.2105x10^{-43}}{3T^3} \cdot \frac{36.25\sqrt{2.25y^2 + x^2}}{\cos 4.304x10^{-67}} \quad (5.22)$$

$$C_{es}^d = \frac{1.2105x10^{-43}}{3T^3} \cdot \frac{36.25\sqrt{2.25y^2 + x^2}}{\cos 4.304x10^{-67}} \quad (5.23)$$

$$C_{es}^d = \frac{4.388x10^{-42}}{3T^3} \cdot \frac{\sqrt{2.25y^2 + x^2}}{\cos 4.304x10^{-67}} \quad (5.24)$$

$$C_{es}^d = \frac{4.388x10^{-42}}{3T^3} \cdot \frac{\sqrt{2.25(26.7)^2 + 0.0667^2}}{\cos 4.304x10^{-67}} \quad (5.25)$$

$$C_{es}^d = \frac{1.1722x10^{-41}}{3T^3} \quad (5.26)$$

$$C_{es}^d = \frac{3.9703x10^{-42}}{T^3} \quad (5.27)$$

The variation of electronic specific heat with temperature (T) for pi and sigma bands is shown with good agreement with experimental data. Using equation (5.27) the variation of electronic specific heat against temperature was studied using Mathcad software and its results tabulated and graph drawn. For electronic specific heat C_{es} , it is determined from the following relation

$$C_{es}^p = \frac{\partial}{\partial T} \frac{1}{N} \sum_p 2(\varepsilon_p - \mu) \langle C_{p\uparrow}^+ C_{p\uparrow} \rangle \quad (5.28)$$

Where ε_b is the energy of π - and σ - bands and μ is the common chemical potential. Using equation (5.28) and putting $\beta = 1/kT$ after simplification, we obtain the following changes where changing the variables as $\varepsilon_p = \hbar\omega_p y, d\varepsilon_p = \hbar\omega_p dy$. Figure 5.2 was gotten.

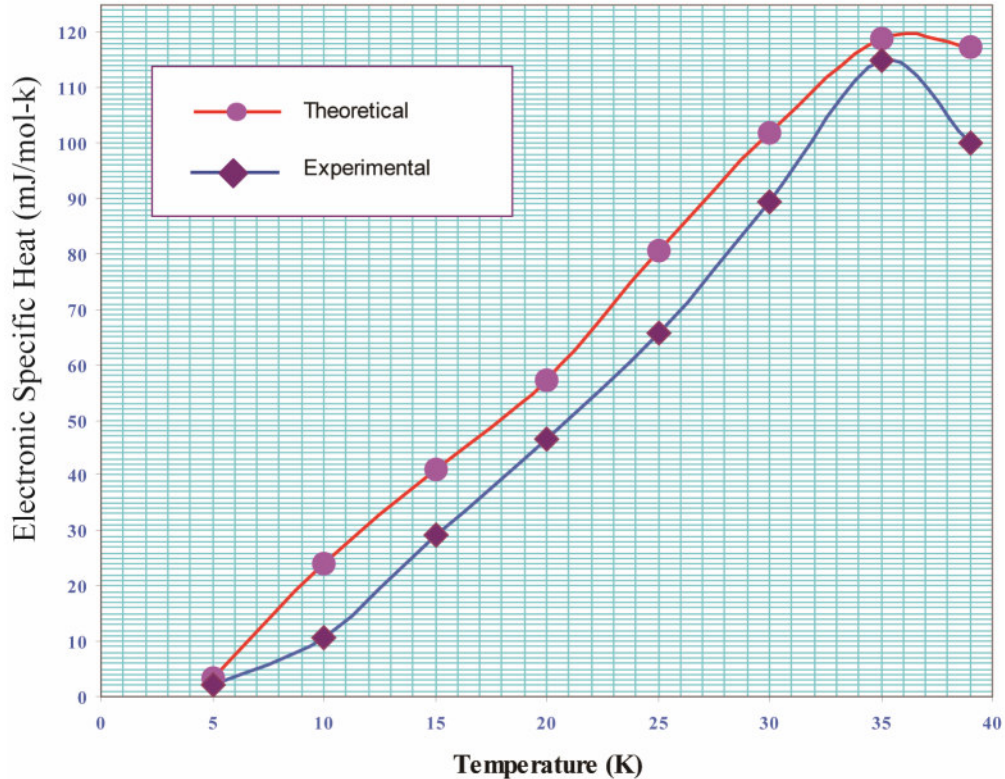


Figure 5.2 Variation of Electronic specific heat with temperature for both p and d bands.

The variation of electronic specific heat C_{es} with temperature T for two bands is shown.

The trend of the graph is nonlinear; there is increase in electronic specific heat C_{es} with increase in temperature. There is a turn in the graph at 35K, with a sharp nonlinear fall in electronic specific heat, signifying optimisity of electronic specific heat.

Theoretical values are higher than experimental for same temperature which can be attributed to mean field approximation method of averaging.

There is a sharp nonlinear fall at 35K in electronic specific heat, signifying optimisity of electronic specific heat.

Graph shows electronic contribution of electrons to heat capacity.

When a metallic system is heated, not every electron gains energy due to equipartition dictates.

Not all electrons are thermally excited as temperature increases

5.1.3 Density of States, D_n and temperature

From equation (4.108)

Where;

D_n is the density of states,

T is the temperature,

U = is the internal energy for one band,

E_n = is the energy for the bands,

K_B = Boltzmann constant and

θ_D = is Debye temperature.

Given that D_n is the density of states, then;

$$T_C = 39K$$

$$U = \text{Range } 3.52 \times 10^{-19} J \text{ to } 1.136 \times 10^{-18} J$$

$$E = 7.2 \times 10^{-3} eV$$

$$= 7.2 \times 10^{-3} \times 1.6 \times 10^{-19}$$

$$= 1.152 \times 10^{-21} J$$

$$K_B = 1.381 \times 10^{-23} J/K$$

$$D_n = \frac{3.52 \times 10^{-19} J}{\int_{1.152 \times 10^{-21}}^{1.136 \times 10^{-18}} \exp\left(\frac{1.152 \times 10^{-21} - 3.52 \times 10^{-19} J}{1.381 \times 10^{-23} J/k(T)}\right) dE}$$

$$D_n = \frac{3.52 \times 10^{-19}}{\int_{1.024 \times 10^{-21}}^{1.152 \times 10^{-21}} (1.152 \times 10^{-21}) \exp\left(\frac{2.541 K}{T}\right) dE}$$

$$T := 0.0001, 0.0002, 10$$

$$D := \frac{3.52 \cdot 10^{-19}}{\int_{1.024 \cdot 10^{-21}}^{1.152 \cdot 10^{-21}} 1.52 \cdot 10^{-21} dE}$$

$$\int_{1.024 \cdot 10^{-21}}^{1.152 \cdot 10^{-21}} \frac{1}{E} dE \rightarrow 4.708856846994461716 \cdot 10^{-23}$$

From Mathcad software

Since E ranges from 6.4eV to 7.2eV which translates to arrange energy of $1.024 \times 10^{-21} \text{J}$ and $1.152 \times 10^{-21} \text{J}$.

Where the equation (4.108) is the variation of density of state D_n and temperature T, for high T_c superconductors in two band models for a system of magnesium diBoride.

Using equation (4.108) the variation of density of states and temperature was studied using Mathcad and the results tabulated and graph drawn.

For the case of density of states function for the pi band is given by

$$\langle\langle C_{p\uparrow} C_{p\uparrow}^+ \rangle\rangle = \frac{(\omega + \epsilon_p)}{(\omega^2 - E_p^2)} \quad (5.18)$$

Where $E_p^2 = \epsilon_p^2 + \Delta_p^2$

When we solve the above equation with partial fraction, we obtain

$$\langle\langle C_{p\uparrow} C_{p\uparrow}^+ \rangle\rangle = \frac{1}{2} \left[\frac{1}{(\omega - E_p)} - \frac{1}{(\omega + E_p)} \right] + \frac{\epsilon_p}{2E_p} \left[\frac{1}{(\omega - E_p)} - \frac{1}{(\omega + E_p)} \right] \quad (5.19)$$

We obtain

$$N_p(\omega) = \frac{1}{2} \sum_p \left[\left(1 + \frac{\epsilon_p}{E_p} \right) \delta(\omega - E_p) + \left(1 - \frac{\epsilon_p}{E_p} \right) \delta(\omega + E_p) \right] \quad (5.20)$$

Changing the summation into integration and after simplification, we obtained

$$\frac{N_p(\omega)}{N_p(0)} = \begin{cases} 2 \frac{\omega}{\sqrt{\omega^2 - \Delta_p^2}} & \text{for } \omega > 0 \end{cases} \quad (5.21)$$

Now using the following values of y , x_1 for Δ_p and x_2 for Δ_d

$$\left(\frac{N_p(0)}{2N_p} \right) = \frac{y}{\sqrt{y^2 - x_1}} \quad (5.22)$$

Similarly, the density of state for pi band is obtained as

$$\left(\frac{N_d(0)}{2N_d} \right) = \frac{y}{\sqrt{y^2 - x_2}} \quad (5.23)$$

The above expressions of density of states function for pi and sigma bands are similar, their behavior has been expressed in the graph.

Density of states is an important function. It helps in interpretation of several experimental data like processes that could occur in crystal but are forbidden because they do not conserve energy.

Some of them take place to correct the energy imbalance by phonon-assisted processes, which will be proportional to $N(\omega)/N(0)$ for $\omega > 0$, the density of states per atom $N(\omega)$ can be defined or

obtained as

$$\left(\frac{N_p(\omega)}{2N_p(0)} \right) = \frac{y}{\sqrt{y^2 - x_1^2}} \quad (5.26)$$

Also, the density of states for σ - band is obtained as

$$\left(\frac{N_d(\omega)}{2N_d(0)} \right) = \frac{y}{\sqrt{y^2 - x_2^2}} \quad (5.27)$$

The above expressions for density of states function for π -and, σ - are similar hence we have evaluated the values with different values of x_1 and x_2 for π - and σ - bands. The behavior of density of states function for both bands is shown in the graph.

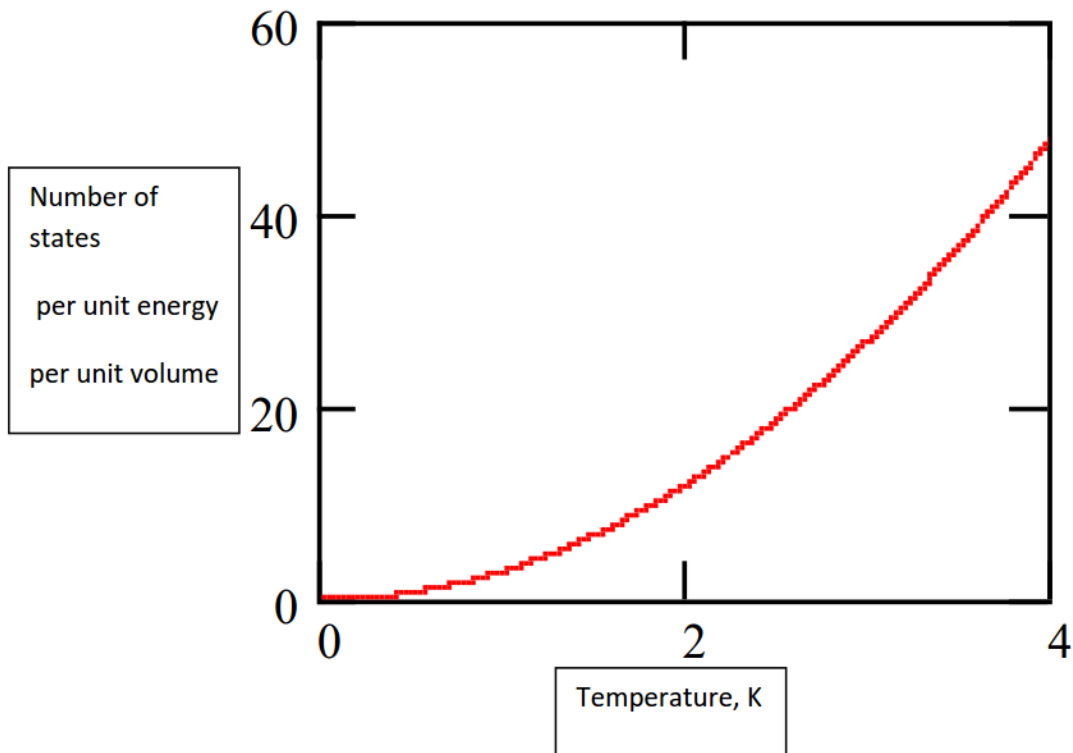


Figure 5.3 Variation of density of state with temperature.

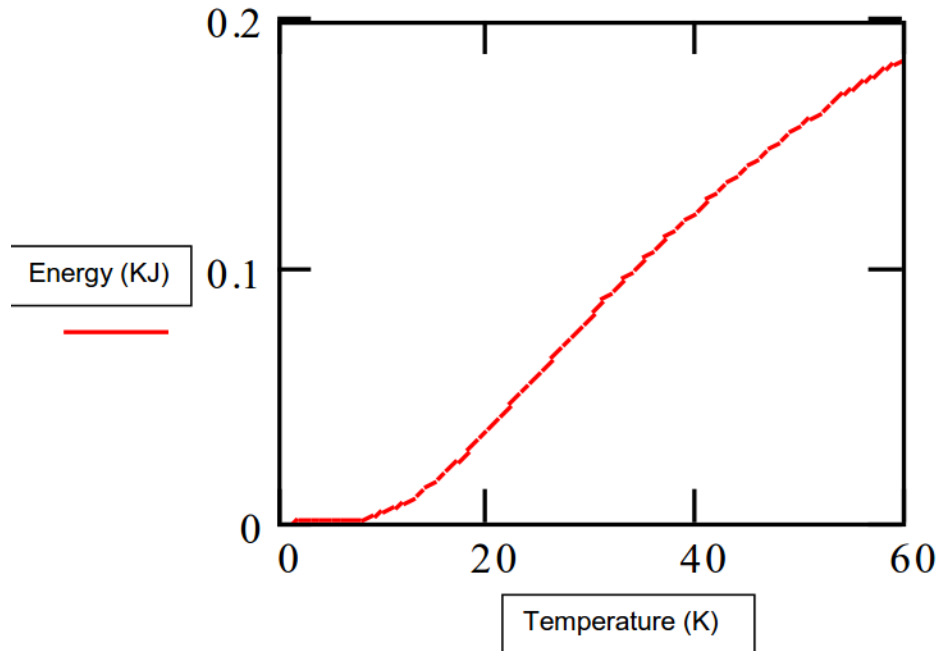
The variation of density of state with temperature T for two bands is shown.

The trend of the graph is nonlinear; there is increase in density of state with increase in temperature.

Variation of density of states function for both with temperature for π - (p holes) and σ - (d holes) bands agrees with experimental data on point contact spectroscopy, specific heat measurement, scanning tunneling and Raman spectroscopy as per (Keimer, Kivelson, Norman, & Uchida, 2015) clearly explains the existence of two distinct superconducting gap with small gaps.

5.1.4 Energy verses temperature

Figure 5.4 Variation of energy verses Temperature.



The trend of the graph is nonlinear, positive gradient with increase in values of energy in Joules with increase in values of temperature in Kelvin.

The graph describes thermal energy between molecules within magnesium diboride system and is a measure of change and a property possessed by the system in a short time. While temperature describes the average kinetic energy of molecules within magnesium diboride system and it is a measurable property of the system also known as a state variable.

5.3 DISCUSSION

Method of calculating transition temperature and inter-band coupling parameter is done. It can be seen that the inter-band coupling effect α is in general a function of μ^*/λ , which is the relative strength of the attractive coulomb interaction μ^* compared to the strength of the inter-band electron-phonon interaction λ . We have illustrated functional dependency and also shown the effect of variation in the electron-phonon inter-band interacting parameter λ_{12} . We found that, by allowing the inter-band electron-phonon parameter to take either positive or negative values, we obtain good analysis.

Values for various parameters in equations obtained above can be used to study parameters for the MgB₂. For superconducting order parameter for MgB₂ system within two band models, we found the following situations; The superconducting parameter for π - and σ - bands, we use the following condition, changing the Variables as $\varepsilon_p = \hbar\omega_p y, d\varepsilon_d = \hbar\omega_d dy$, when solved numerical, we study the variation of superconductivity order parameters Δ_p and Δ_d with temperature corresponding to π -and σ - bands. The behavior of superconducting order parameters corresponds with temperature as in the shown curve. The superconducting order parameter for combined π - and σ - bands can be studied by taking a simple sum of both the parameters. Taking the sum of order parameter $\Delta = \Delta_{\pi} + \Delta_{\sigma}$ one can obtain the values by solving numerically. A comparison of order parameter with BCS type curve was shown in the graph.

CHAPTER SIX CONCLUSIONS AND RECOMENDATION

6.1 CONCLUSIONS.

In the search for a suitable method of explaining thermodynamic properties of high T_C superconductors in two band models, we have shown the study of superconducting in MgB_2 by canonical two band BCS Hamiltonian containing Fermi surfaces of p and d bands. The envisaged interaction of phonon mediated attraction and coulomb repulsion was proposed to act differently on energy band states and stabilizing superconductor phase for MgB_2 to unearth the mystery of microscopic mechanisms that allow superconductivity to persist at such high temperatures.

Following Bogoliubov -Valatin technique and equation of motion method, we have obtained the expressions for electron-phonon interaction model Hamiltonian for two band model isotope, expression for variation of thermodynamic properties with temperature and expression for variation of order parameter and transition temperature T_C , which were the objectives of the study. Using the values of various parameters for a system MgB_2 , we have made study of various physical properties and wherever possible, compared our results with available experimental data.

The statistical thermodynamics of high T_C superconductors in two band model by considering interaction of phonon mediated attraction and coulomb repulsion it achieved its objectives by formulating an effective Hamiltonian given by equation (4.60) as diagonalized equation by Bogoliubov-Valatin transformation equations, energy of the system given by (4.76), specific heat capacity equation (4.84), entropy given in equation (4.97) and expression for transition temperature T_C given in equation (4.99).

Ground state energy was obtained from the diagonalised Hamiltonian using Bogliubov-volatin transformations. Thermodynamic properties of high T_c superconductor namely heat capacity, energy, entropy and critical temperature were determined.

The transition temperature T_c , which is a function of energy could be raised by varying phonon energy ε_{pd} .

The calculated values of

$$C_V=0.0192729906\text{eV/K},$$

$$T_C=47.667720441\text{K},$$

$$E_g=0.4111340888\text{eV}$$

$$E_g=0.7670001738\text{eV and}$$

$S= 3.3245572813\text{eV/K}$, are in agreement with results from other authors and predicted higher T_C for electron- phonon mediated for both p and d bands.

1. The predicted transition temperature for system MgB_2 varied from 39K to 47.667720441K.
2. The temperature dependent on two superconducting gaps Δ_p and Δ_d corresponding top and d bands for MgB_2 was found. The two gaps structure is perfectly in agreement with experimental observations and values.
3. The specific heat behavior obtained from our model verses Temperature is in satisfactory agreement with experimental results, although the theoretical values are slightly higher than the experimental values which are attributed to mean field approximations.
4. The density of states behavior is similar to BCS weak coupling superconductors corresponding p and d bands. There is a marked difference between the two curves. This reveals that MgB_2 superconductors in this respect resembles to that of high T_C cuprates but the density of states for the system MgB_2 is quite high.

The main objective and specific objectives were achieved with the results agreeing in principle with other authors and researchers.

6.2. RECOMMENDATIONS

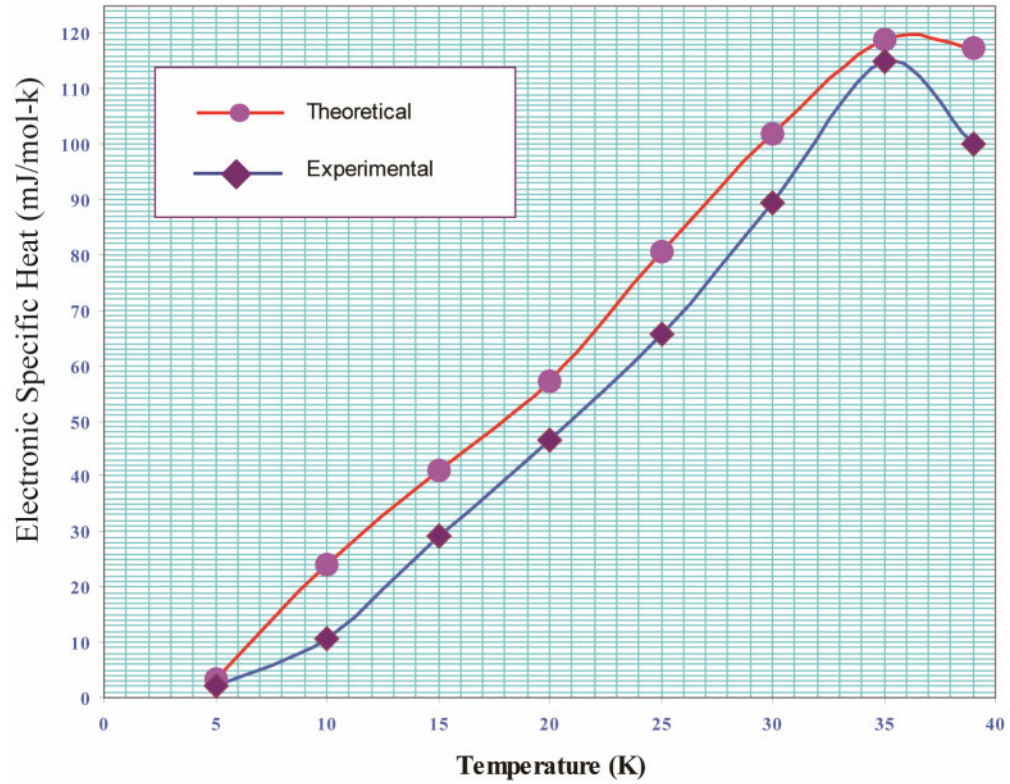
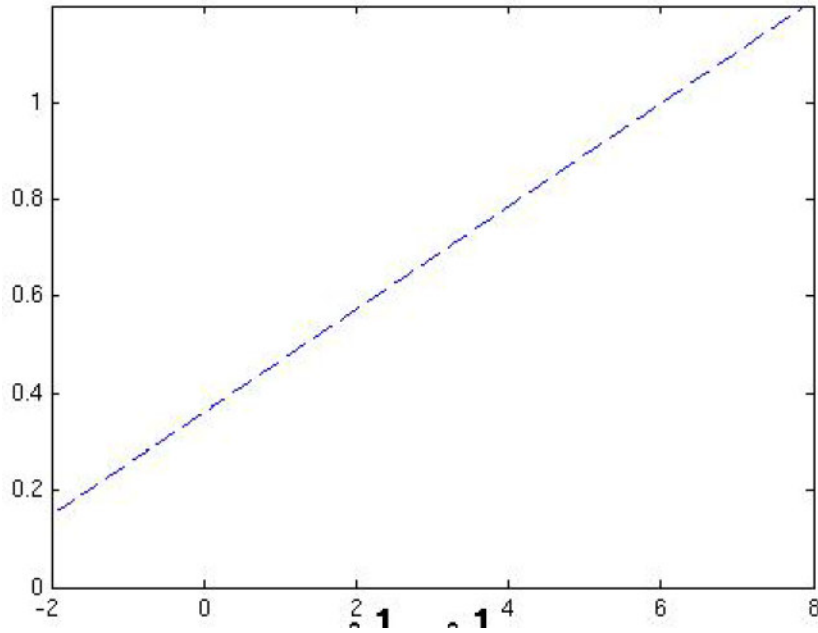
Our model shows reasonable agreement with available data. The mechanism emerges as a strong contender for acceptable two bandmodel for MgB_2 , non cuprate high- T_C superconductor. The efforts in determining the pairing mechanism in this system need to continue, for such efforts go hand in hand with enhancing future prospects for new HTSC material and novel applications.

REFERENCES

- Akimitsu, J. (2001). *Symposium on Transition Metal Oxides*. Sendai, Japan.
- Allan, M. P. (2013). *Imaging Cooper Pairing of heavy fermions in CeCoIn₅*. *Nature Physics*.
- Bednorz, J. G., & Mueller, K. A. (1986). *Possible high T_c Superconductivity the Ba-La-Cu-O system*. *Zeitschrift fuer Physik* .
- Bogoliubov. (1947). *On the theory of superfluidity, J. Phys. (USSR), 11, p. 23 , (Izv. Akad. Nauk Ser. Fiz. 11, p. 77 .*
- Bogoliubov, & Valatin. (1958). *Canonical transformation for interacting system* .
- Choi, H. J., Roundy, D., Sun, H., & Cohen, M. L. (2002). The origin of the anomalous superconducting properties of MgB₂. *Nature*, 418(6899), 758-760.
doi:<https://doi.org/10.1038/nature00898>
- Hensen, S., Mueller, G., Riek, C. T., & Scharnberg, K. (1997). *In plane surface impedance of epitaxial films: comparison of experimental data taken at 87 GHz with wave models of superconductivity, Physics review B 56:6237.*
- Kaindl, A. R., Orenstein J, Carnahan , M. A., Chemla, D. S., Lowndes, D. H., Christen, H. M., . . . Paranthaman, M. (2001). *Preprint, Far-infrared optical conductivity gap in superconducting MgB₂ films.*
- Keimer, B., Kivelson, S. A., Norman, M. R., & Uchida, S. (2015). from quantum matter to high-temperature superconductivity in copper oxides,. *Nature*, 518:179-186.
- Keisuke, & Dasuke, Y. (2012). Cooper Pairing of Fermions with un equal masses in Heavy-Fermion Systems. *Journal of the Physical Society of Japan*, 81.
- Keisuke, Y., & Daisuke, M. (2012). Cooper Pairing of Fermions with Unequal Masses in Heavy-Fermion Systems. *Journal of the Physical Society of Japan, The Physical Society of Japan,, Vol. 81, SB010 .*
- Legget, A. J. (2006). *What DO we know about high T_c? Nature Physics.*
- Martins, P. B. (2006). *New topics in superconductivity research*,. New York: Nova Science publishers.
- Mathias, B. T., Geballe, T. H., & Corenzwit, E. (1950). *Superconductivity of Nb₃ Sn. Physical Review.*
- Mourachkine, A. (2004). *Room-Temperature Superconductivity*. Cambridge.
- Onnes, H. K. (1911). *The superconductivity of mercury*. *Comm. Phys. Lab. Univ.*
- Poole C P Jr, C. P. (2000). *Academic. Superconductor types, in Handbook of superconductivity, pp.71. San Diego: Poole C P Jr (eds.) Press.*
- Possible high T_c Superconductivity the Ba-La-Cu-O system.* (n.d.).
- Rapando, B. W., Khanna, K. M., & Mong'are, P. A. (2016). The diagonalised T-J Hamiltonian and thermodynamic properties of High TC superconductors. *American Research journal for physics. Volume 2016.*
- Schrieffer, J. (2013). *Superconductivity; Discoveries and Discoveries*. Berlin: Springer Overlag.
- Sethna, P. J. (2012). *Statistical Mechanics : Entropy , Order parameter and Complexity*. Oxford: Clarendon Press.
- Tinkham, M. (2004). *Introduction to superconductivity,2nd ed Mchill.*

Valatin, J. (1958). *Comments on the theory of superconductivity*. Nuovo Cim.

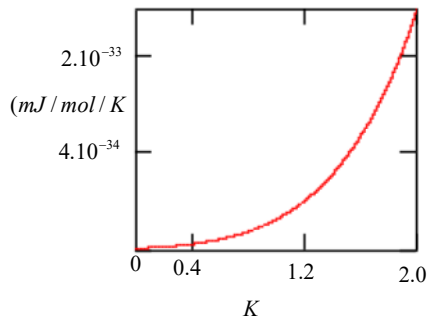
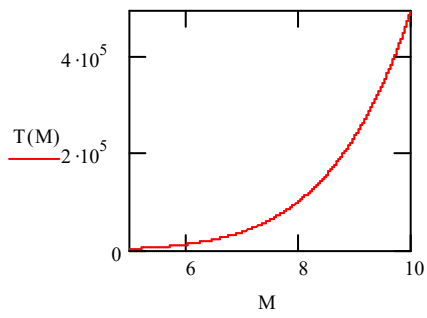
APPENDICES.



C := 0.001, 0.002..3

T := 0.001, 0.002..2

$$C(T) := \frac{3.907 \cdot 10^{-42}}{T^3}$$



φ := 10, 15..40

T := 10, 25..50

$$\phi := \frac{3.52 \cdot 10^{-19}}{4.7088 \cdot 10^{-23} e^{\left(\frac{2.541}{T}\right)}}$$

E := 0.001,0.002..5

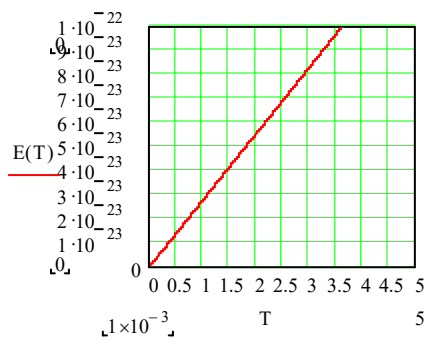
T := 0.001,0.002..5

E(T) := 2.76 · 10⁻²³ · T

E := 0.001,0.002..5

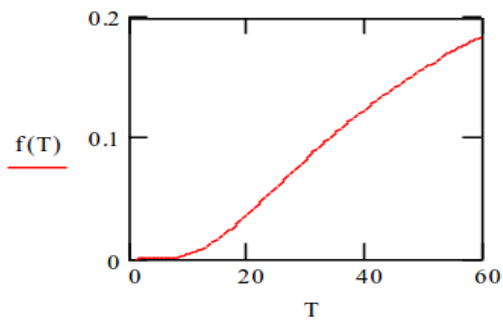
T := 0.001,0.002..5

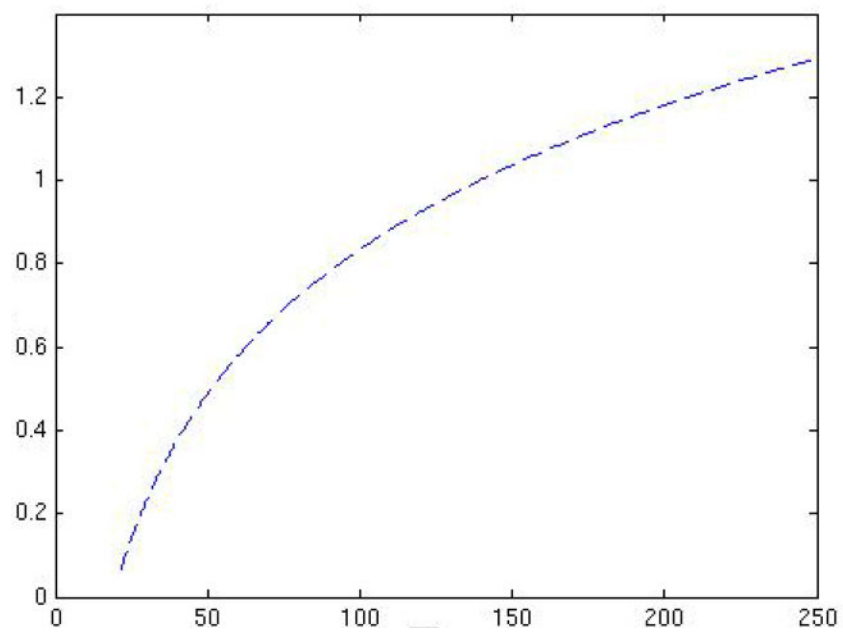
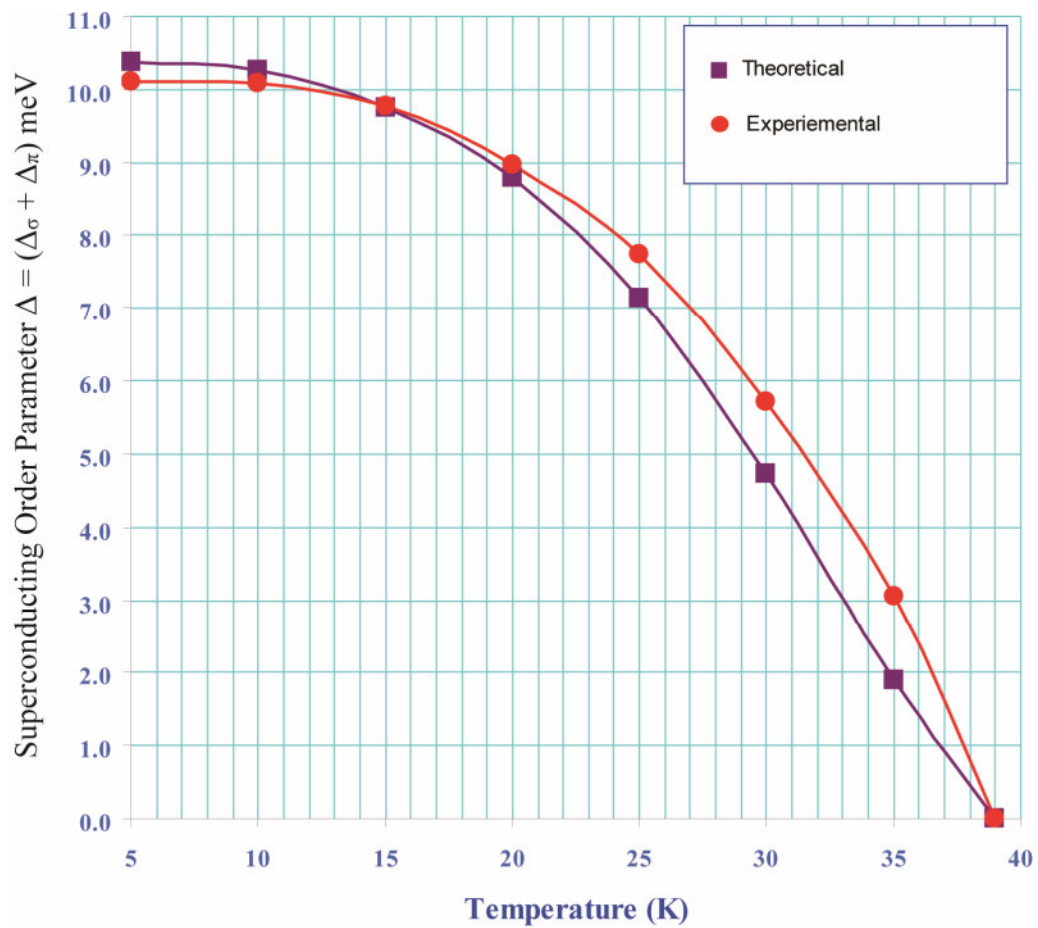
E(T) := 2.76 · 10⁻²³ · T



f(T) := 0.411e ^{$\frac{-47.666377}{T}$}

T := 0..60





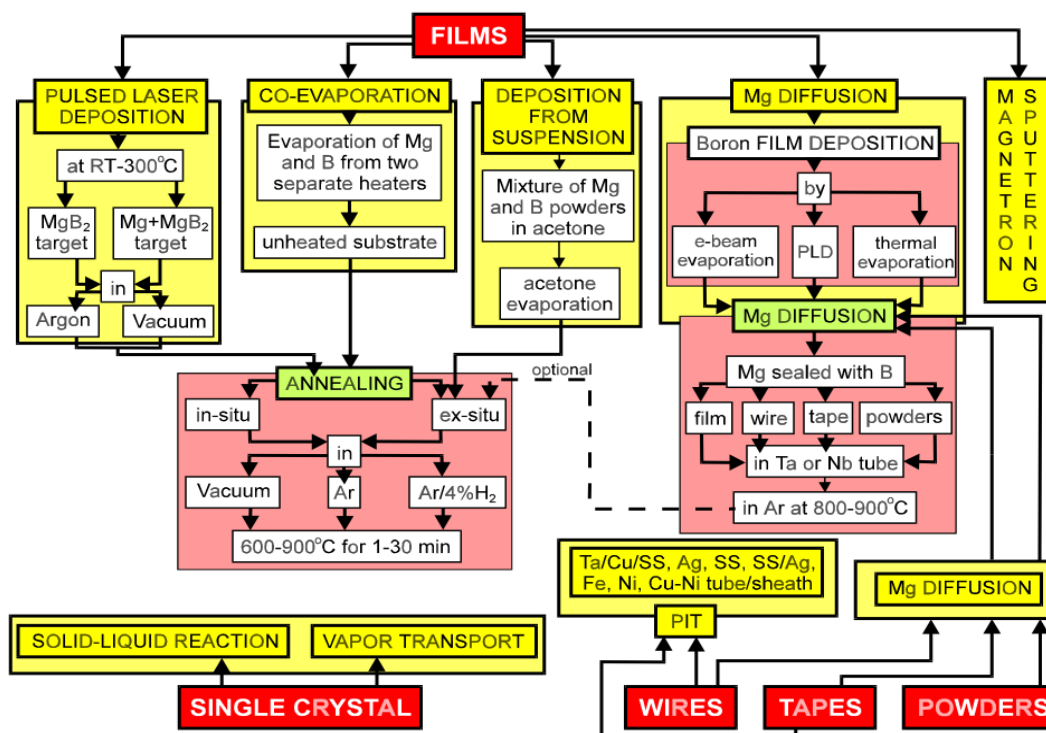


Table 2.4: Schematics of experimental methods of preparation for MgB₂. (Poole C P Jr, 2000)

S. No.	Parameter	Value
1	Superconducting transition temperature (T_c)	39 K
2	Phonon energy ($\hbar\omega_p$) for p holes	0.00937 eV
3	Phonon energy ($\hbar\omega_p$) for d holes	0.00875 eV
4	Density of states at the Fermi surface $N(0)$	$\cong 3.093 \times 10^{18}$ eV/atom
5	Pairing interaction for p holes (V_p)	$\cong 3.093 \times 10^{18}$ eV/atom
6	Pairing interaction for d holes (V_d)	$\cong 3.093 \times 10^{18}$ eV/atom
7	Pair interchange between two bands (V_{pd})	1.80 eV
8	Number of atoms per unit volume	$\sim 5 \times 10^{22}$
9	Crystal Structure	Hexagonal
10	Cell Parameter	$a = 3.086 \text{ \AA}, c = 3.524 \text{ \AA}$
11	Boltzmann constant (k_B)	0.00008625 eV/K
12	Electron Mass (m_e)	9.1×10^{-31} kg

Table 2.3 Values for various parameters for MgB₂ system. (J. Nagamatsu *et al* 2001)